Computational Modeling and Analysis of Mechanically Painful Stimulations

Manafi Khanian, Bahram

DOI (link to publication from Publisher):
10.5278/vbn.phd.med.00010

Publication date:
2015

Document Version
Publisher's PDF, also known as Version of record

COMPUTATIONAL MODELING AND ANALYSIS OF MECHANICALLY PAINFUL STIMULATIONS

BY
BAHRAM MANAFI KHANIAN

DISSERTATION SUBMITTED 2015

AALBORG UNIVERSITY
DENMARK

Computational Modeling and Analysis of Mechanically Painful Stimulations

PhD Thesis

Bahram Manafi Khanian

Center for Neuroplasticity and Pain (CNAP), SMI®
Department of Health Science and Technology
Aalborg University
Denmark

Thesis submitted: August 2015

PhD supervisor: Professor Lars Arendt-Nielsen

PhD committee: Associate Professor Carsten Dahl Mørch (chairman)
Aalborg University, Denmark

Dr. Sebastian Dendorfer
Ostbayerische Technische Hochschule Regensburg, Germany

Dr. Dagfinn André Matre
National Institute of Occupational Health, Norway

PhD Series: Faculty of Medicine, Aalborg University

ISSN (online): 2246-1302
ISBN (online): 978-87-7112-343-2

Published by:
Aalborg University Press
Skjernvej 4A, 2nd floor
DK – 9220 Aalborg Ø
Phone: +45 99407140
aauf@forlag.aau.dk
forlag.aau.dk

Printed in Denmark by Rosendahls, 2015

Preface

The PhD studies were carried out at Center for Sensory-Motor Interaction (SMI), Aalborg University, Denmark, in the period from 2013 to 2015. This dissertation is based on the following three peer-reviewed articles. In the text these are referred to as study (I) to (III) (Full-length articles in Appendix).

Study I

Paper 1: Deformation and pressure propagation in deep somatic tissue during painful cuff algometry; Bahram Manafi-Khanian, Lars Arendt-Nielsen, Jens Brøndum Frøkjær, Thomas Graven-Nielsen. *European Journal of Pain 2015.*

Study II

Paper 2: An MRI-based leg model used to simulate biomechanical phenomena during cuff algometry: A finite element study; Bahram Manafi-Khanian, Lars Arendt-Nielsen, Thomas Graven-Nielsen. *Medical & Biological Engineering & Computing 2015.*

Study III

Paper 3: Interface pressure behavior during painful cuff algometry; Bahram Manafi-Khanian, Lars Arendt-Nielsen, Kristian Kjær Petersen, Afshin Samani, Thomas Graven-Nielsen. *Pain Medicine* (submitted April 2015)

Abstract

Cuff algometry is used for quantitative assessment of deep-tissue sensitivity. The mechanical pressure is transmitted to the deep-tissues through the superficial layers, exciting deep-tissue nociceptors and eventually initiating pain sensitivity. The mechanical influences of a circumferentially distributed pressure which is applied by a tourniquet during cuff algometry on deep-tissue nociceptors are not clarified. It is unknown which anatomical tissues are mainly excited and how the generated stress and strain are propagated in deep-tissues during cuff stimulations. The characteristics of the pressure distribution exerted on the limb surface are of the significant factors in provoking deep-tissues during cuff algometry methodology. However, the knowledge on the features of this interface pressure and its effect on pain response are lacking. For this purpose, three studies, providing a novel insight into the intrinsic and extrinsic factors involving mechanically induced pain by cuff pressure algometry, were performed.

Three-dimensional finite element model of the lower leg was developed based on MRI data to extract the stress and strain distribution in deep tissues during different cuff compression intensities. The pressure between the cuff and skin was measured and characterized to describe the pattern of interface pressure which is truly applied on the limb surface during painful cuff algometry. In study (I), the stress and strain distribution in various anatomical structures generated by cuff compression, were reported. This study described the efficacy of cuff stimulation methodology for activation of deep-tissue nociceptors. The stress and strain originate from the areas in the vicinity of hard tissues and are propagated toward the outer layers of muscle tissue. Moreover, assuming strain as the ideal factor for stimulation of nociceptors, the outcomes of study (II) suggested that cuff algometry is more capable to challenge the nociceptors of superficially muscle structures compared with the periosteal tissues located in the proximity of bony structures. The results of study (III) confirmed that the magnitude and distribution of interface pressure between the cuff and limb are of the crucial factors determining pain response. The homogeneity of interface pressure could be improved using a liquid medium between the cuff and limb although this can cause a significant decline in the amount of interface pressure.

The present findings are highly relevant to biomechanical studies for defining a valid methodology to appropriately activate deep-tissue nociceptors and hence to improve the reliability of cuff algometry data which are useful in clinical studies.

Abstrakt (abstract in Danish)

Cuff-algometri bliver brugt til at kvantificering af musklers smerte sensitivitet. Det mekaniske tryk bliver transmitteret gennem de overfladiske vævslag og eksitere de dybtliggende receptorer og igangsætter til sidst smertesensitiviteten. Den mekaniske indflydelse af periferisk distribueret tryk, som bliver påført af en manchet ved cuff-algometri af de dybtliggende receptorer, er ikke klarlagt. Det vides ikke hvilket anatomisk væv, der hovedsagligt aktiveres, og hvordan belastning og spænding propagerer i det dybtliggende væv under cuff stimulationer. Karakteristikken af trykfordelingen der bliver påført en vævets overflade er en signifikant faktor, der påvirker de dybere liggende væv ved brug af cuff-algometri. På trods af dette, er der stadig manglende viden omkring karakteristika af grænsefladetrykket og dens påvirkning på smerteresponset. Derfor er der blevet lavet tre studier, der giveindblik i indre og ydre faktorer, der er involveret i mekanisk-induceret smerte ved brug af cuff-algometri.

3D finite element modeller blev udviklet af underbenet baseret på MRI-data for at udtrække spændings- og belastningsfordelingen af dybtliggende væv under forskellige manchet-kompressionsintensiteter. Trykket mellem manchetten og huden blev målt og karakteriseret for at beskrive mønsteret af grænsefladetrykket, som reelt er påført ekstremitetens overflade under smertefuld cuff-algometri. I studie (I) blev spændings- og belastningsdistributionen i forskellige anatomiske strukturer rapporteret under manchet-kompression. Studiet viste at cuff-algometri er en mere effektiv tilgang til at aktivere dybtliggende smertereceptorer. Ligeledes blev det vist at mængden af spænding og belastning var koncentreret omkring knogler med udstrålinger ud til muskelvæv. Derudover, hvis belastining antages at være den ideelle faktor for at stimulere smertereceptorerne, tyder resultaterne af studie (II) på at cuff-algometri er bedre i stand til at stimulere smertereceptorer i øvre muskelstrukturer sammenlignet med periostealt væv, beliggende omkring knoglen. Resultaterne fra studie (III) bekræftede at størrelsen og distributionen af grænsefladetrykket mellem manchetten og vævet er vigtige faktorer for at bestemme smerteresponset. Ensartetheden af grænsefladetrykket kan forbedres ved brug af et flydende medium mellem manchetten og vævet, selvom dette forårsagede et signifikant fald i grænsefladetrykket.

Disse fund er særdeles relevante for biomekaniske studier til at definere valide metoder til korrekt aktivering af dybtliggende smertereceptorer og dermed forbedre pålideligheden af cuff-algometri måling, for at forbedre brugbarheden i kliniske studier.

Acknowledgements

I would like to acknowledge my principal supervisor, Prof. Lars Arendt-Nielsen for the inspiring and fruitful discussions, and his substantial supports. Furthermore, I would like to express my gratitude to Prof. Thomas Graven-Nielsen for his valuable comments on my projects and providing positive feedbacks in different studies.

I would also like to thank all staffs from the department of Health Science and Technology (HST) at Aalborg University. My gratitude is particularly extended to Associate Prof. Afshin Samani for his significant contribution to my studies.

Finally, I would like to appreciate my family who consistently supported me.

This study was supported by a proof-of-concept grant from the Ministry of Higher Education and Science, Denmark. EIR and SMI are acknowledged for providing facilities for this project.

Contents

Chapter 1

Introduction

This chapter provides a concise overview of the backgrounds to clarify the potential studies of the present project. The fundamental aims of the dissertation are also presented.

1.1. Musculoskeletal pain

An abundance of research demonstrates that chronic pain imposes a substantial burden on sufferers, the health care system, society, and the economy [41,76,86] because pain is the most frequent cause of productivity loss [7,29,86], the main reason of health care utilization [18,27,40,85], and strongly associated with a poor quality of life [18,56,86]. The musculoskeletal pain is more prevalent than superficial pain and about 23% of pain patients suffer from muscle and deep tissue pain [40]. The implications of experimental pain approaches are highly relevant to clinical studies for pain sensitivity assessment and pain mechanisms. The experimental pain can be evoked by two methods. Endogenous methods induce deep-tissue pain by physiological stimuli such as strong exercise or ischemia, while exogenous methods involve external stimuli such as pressure stimulation or infusion of algesic substances [79]. Nociceptors can be found in skin (cutaneous nociceptors), muscle, and viscera [61]. The nociceptive afferents of deep-tissue are poly-modal confirming their sensitivity to thermal, chemical, and mechanical stimulations [54]. Acute musculoskeletal pain occurs in response to each kind of mentioned excitations of deep-tissue nociceptors transducing the stimuli into neural signals and supplied by group III and IV afferent fibers [61]. Spatial and temporal summation [69] and factors determining the stimulus intensity such as strength, volume, and concentration mainly contribute to the muscle pain sensation [33]. Pain can be aroused from deep fascia, periosteal tissue, and tendons [84]. The term *muscle pain* is used for pain originating from muscle tissue including its fascial tissue and tendons [61]. The pain localization in deep tissue is poor and it is difficult to be differentiated between the pain sources [32]. It is typically experienced referred pain from muscle in deep tissue i.e. muscles or joints, while referred pain from visceral structures is often felt in both deep and superficial tissues [53].

1.2. Pain sensitivity assessment

Quantification of sensory assessment of musculoskeletal pain needs standardized technologies for both stimulation of deep tissue nociceptors and quantitative assessment of pain sensation [32]. It has been shown that mechanical pressure applied on muscle tissue is an appropriate method to evaluate the tissue sensitivity thresholds [2,48]. The pressure is transmitted into the deep structures via the skin and subcutaneous adipose layers, inducing pain by excitation of deep-tissue nociceptors [34]. The pressure algometer is a valid device for musculoskeletal pain sensitivity assessment [26]. A pressure algometer is a force gauge with different cylindrical probe size and probe shapes by which the pressure needed to evoke musculoskeletal pain can be exerted and recorded. It has been suggested that several factors may affect the measurement of pressure algometry. The extrinsic factors like examiner skills [35,37,62], probe dimension and probe shape [24], temporal aspects [23] and also intrinsic factors such as tissue type [71], muscle hardness [21], and thickness of subcutaneous adipose layer [25] can potentially influence the pressure pain threshold and pressure pain tolerance. The procedure of applying pressure to elicit musculoskeletal pain can be manual or computer-controlled. Manual algometry has been clinically used to investigate pain responses in various patient conditions e.g. whiplash [51,78], osteoarthritis [1], and headache [72]; however, the pressure rate and the measurement results might be biased due to the visual feedback which is dependent to examiners skills [20]. The inherent variability associated to manual involvement of the examiner is excluded using the computer-controlled pressure algometry. Computerized pressure algometry increases measurement reliability by controlling localization, and pressure rate which guarantees stable stimulus configuration [70]. Also, recording the pain intensity continuously on a visual analogue scale (VAS) is possible in computerized pressure algometry. This recording allows that the stimulus-response function between the applied pressure and pain intensity to be evaluated.

In single-point pressure algometry the stimulation probe is typically 1 cm^2 meaning that a restricted volume of tissue is stimulated by this technique [24]. Alternatively, cuff algometry is a stimulation technique challenging more structures over a larger area and is not significantly influenced by local variations of pain sensitivity [49,70]. In computer-controlled cuff algometry, a pneumatic tourniquet is wrapped around an extremity and inflated using different pressure paradigms e.g. ramp, stepwise, and periodic function. Pain detection thresholds (PDT), pain tolerance threshold (PTT), and stimulus-response function can be recorded for assessment of pain response and deep-tissue pain sensitivity [32,70]. The

methodology of cuff pressure algometry has also been used to quantify the pain sensitivity in the lower leg of healthy subjects [70], patients with osteoarthritis before and after total knee arthroplasty [75], and patients with fibromyalgia [49]. Cuff stimulation applied on the limb elicits the pain sensitivity from the superficial and deep tissues; however, it has been shown that the deep-tissue nociception is the major component of evoked pain in pressure algometry [34].

1.3. Modelling of painful pressure algometry

Finite element (FE) analysis is a computational and reliable technique for evaluation of the mechanical parameters of physical systems where an analytically exact approach is not feasible [73]. It is extensively used in biomedical engineering for simulation of biological tissues under any kind of loading conditions. Theoretically, the biomechanical aspects of the tourniquet cuff have been studied [38]. Axisymmetric finite element analysis has been used to simulate the tourniquet application on limb [3]. Cylindrical finite element modelling has also been performed to investigate the influences of cuff compression on venous blood flow [15] and cross sectional area of the vessels [64]. The finite element method has also been used to simulate the effects of single-point algometry on structural mechanical properties in deep-tissues [21] while there is highly limited knowledge about how the biomechanical stress and strain is distributed in superficial and deep tissues during painful cuff algometry.

There is an investigation using the finite element method to show the relationship between the pressure-induced muscle pain and tissue biomechanics in lower leg during the single-point algometry with different probe sizes and shapes [24]. It has been demonstrated that probe design and diameter play an important role in the distribution of stress and strain in tissues; larger and rounded probes are more efficient to generate muscle strain which is mainly related to muscle pain whereas smaller and flat probes mostly challenge superficial structures [24]. In single-point pressure algometry the skin layer was subjected to the higher amount of stress and lower amount of strain confirming the protective role of skin for the inner structures [24]. Based on this it has been suggested that the mechanosensitivity of deep-tissue nociceptors is lower than the superficial nociceptors or alternatively the mechanical sensitivity of deep-tissue nociceptors is related to strain rather than stress [21,24]. So far there is limited information about the stress and strain distribution in deep and superficial tissues during painful cuff algometry. The main differences between the stress and strain distribution

of single-point algometry and cuff algometry and how these two techniques affect the deep-tissue nociceptors remain unclear.

The pathogenesis of bone-associated pain and appropriate treatment remain a challenge [17]; however, it has been shown that the periosteal layers of hard tissues are densely innervated by sensory fibers [59] and are sensitive to mechanical stimulations [39,43]. Using advanced imaging techniques it has been proposed that sensory fibers innervating the periosteal layers are ideally organized to detect mechanical distortion of the bone [60]. Mechanical and chemical stimulations of the periosteum at the tibia bone caused pain [42,57]. Infusion of hypertonic saline into the region around the bony structure was more painful than when applied to other tissues such as subcutaneous adipose and muscle [36]. Also, mechanical stimulation of the periosteal layers imposed a significantly lower painful pressure thresholds compared to stimulation of the tendons, ligaments, fibrous capsule, fascia, and muscle [60]. These findings confirm the substantial role of periosteum in association with bone pain. A finite element model has been developed to simulate the stress and strain distribution in tissue covering the tibia bone when the single-point algometer with different probe sizes was applied on the tibial bone site [22]. The painful pressure threshold and corresponding indentation value were significantly lower with the small probe compared to the larger probes. Smaller probes were more efficient to cause a high strain in the periosteal tissue compared to the larger probes and hence it has been suggested that small probes are more capable to evoke bone-related pain [22]. Cuff pressure algometry is clinically used for profiling of patients with various musculoskeletal pain conditions [49]; however, there is limited information to show that which tissues are particularly excited by this method. There is an essential need to evaluate the influences of cuff compression on structural mechanical properties at the proximity of bony structures representing the periosteal tissue in contrast with more superficially located muscle structures to assess the capability of cuff methodology for evoking various kinds of pain e.g. bone pain and muscle pain. The outcomes would be potentially helpful in pharmacological profiling and diagnostic procedure of bone-associated pain.

A three-dimensional finite element model of the calf has been developed based on MRI data to assess the stress and strain values in muscle compartment during single-point pressure algometry on the tibialis anterior and gastrocnemius muscles [21]. It has been proposed that pressure pain thresholds were significantly higher for the gastrocnemius muscle stimulation compared to the tibialis anterior stimulation. Finite element simulations have also represented

that the strain in superficial muscle was higher and more widespread for stimulation on the gastrocnemius muscle compared with the stimulation on the tibialis anterior muscle at painful pressure thresholds [21]. It has been hypothesized that these differences might be related to variations in the mechanical properties of tibialis anterior and gastrocnemius muscles which explain that a more stretchable muscle e.g. the gastrocnemius is softer, while a less stretchable muscle e.g. the tibialis anterior is harder [21,55]. Human tissues are anisotropic and inhomogeneous [28] meaning that their mechanical properties are dependent on orientations and locations [11]. Moreover, various anatomical structures composing the limb show different biomechanical responses to the external stimulations. These factors as well as the irregularity of the limb geometry could result in different painful pressure thresholds depending on stimulation site in single-point pressure methodology. Thus, the pain sensitivity thresholds during cuff algometry might be related to the uniformity of pressure distribution being applied on the limb. So far, no studies have shown whether the painful pressure values are influenced by changing the uniformity of interface pressure. In an air cuff the highest pressure occurs under the middle of the cuff and the lowest pressure is under the cuff edges suggesting that this pressure gradient generates shear effects inside the limb [31]. Changing the interface media from e.g. air to water might moderate this unfortunate shear force characteristics in cuff methodology. However, there is limited information about the differences of interface pressure distribution between the water-cuff and air-cuff. Water is incompressible compared with the air and use of a liquid interface between the limb and cuff would modify the homogeneity of interface pressure distribution. Thus a detailed understanding of the characteristics of interface pressure distribution i.e. magnitude, and homogeneity and their relationship with pain response may lead to an improvement in the design of cuff algometry system for providing more reliable data.

1.4. Aims of the PhD project

The overall aim of this thesis was to provide a new insight into the intrinsic and extrinsic factors which are involved in mechanically induced pain during cuff pressure algometry. To investigate these factors, a computational finite element model of the lower leg was developed to quantify the mechanical parameters and evaluate stress and strain distributions in different anatomical structures composing the limb at various cuff compression intensities. Study I gained insight into the capabilities of cuff algometry in terms of the stress and strain

generation in superficial and deep tissues. Study II followed the methods in study I to assess the capability of cuff algometry in activation of nociceptors of the periosteal layers compared to the more superficial muscle structures.

In study III the magnitude and homogeneity of interface pressure which actually exists between the cuff and limb and also the influences of using a liquid medium on the characteristics of interface pressure distribution in cuff algometry systems were investigated. The overview of the performed studies is illustrated in Figure 1.

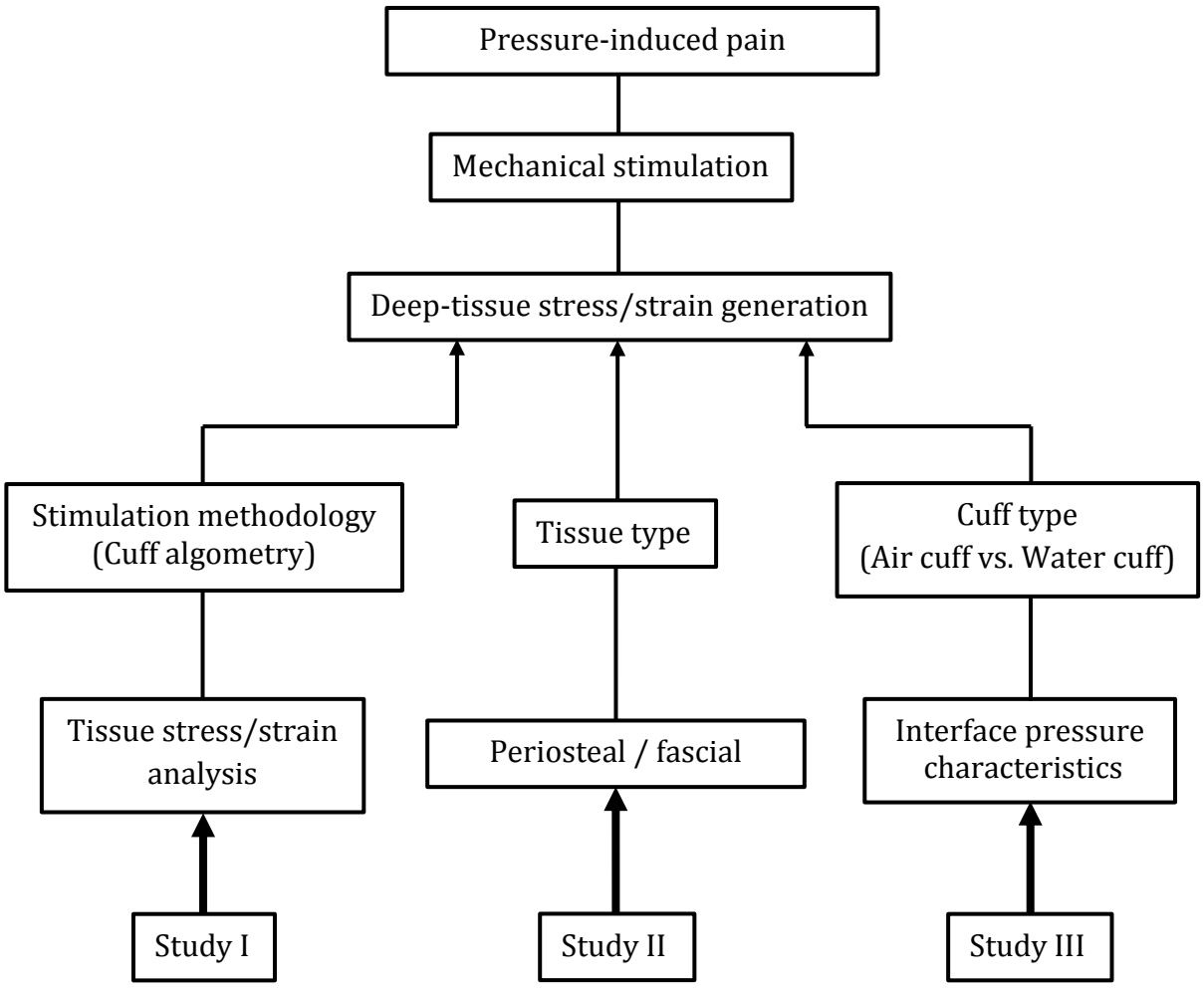

Figure 1. Schematic representation of the PhD project investigating mechanical factors involving pain sensitivity assessment during cuff algometry.

Chapter 2

Biomechanics of human tissues

This chapter presents a general overview of the principal concepts of mechanics of materials and different models which are commonly used for simulation of the behavior of human soft tissues. The finite element method which is extensively used for computational simulation of biological tissues has also been clarified in this chapter.

2.1. Fundamental mechanics of materials

In continuum mechanics, stress is a physical quantity that expresses the internal force field in a continuous material which is subjected to an external loading [11]. In structural mechanics the external loading can be found in various forms such as axial loading (tension or compression), bending, torsion, and transverse loading [80]. The normal stress (σ) in a simple uniaxial loading is defined as the magnitude of applied force divided by the cross sectional area perpendicular to the force direction whereas the shear stress (τ) is the force value divided by the area parallel with the force direction. The stress is calculated by the more complex formulas in condition that the applied load is not simple; however, it generally represents the average force per unit area of a surface within a deformable body [77]. The SI unit of stress is the same as that of pressure (Pa). From the view point of structural mechanics, pressure is the special case of loading when the normal stresses along the Cartesian axes are compressive and equivalent in magnitude and the shear stresses are zero [80].

Strain is a normalized dimensionless quantity that represents the internal deformation and displacements between the particles in a deformable body [58]. In the case of uniaxial loading the strain is defined as the variation of length divided by the original length and is usually expressed as a decimal fraction [77]. In many materials, the relationship between the applied stress is directly proportional to the resulting strain up to a certain limit and the slope of this linear relationship is known as modulus of elasticity whereas most of biological tissues act as the non-linear materials.

In a general case of loading the Cauchy stress tensor of an element inside the body is a second order tensor which is used for stress analysis of the materials experiencing small deformations [45].

$$\text{Cauchy stress tensor} = \sigma_{ij} = \begin{bmatrix} \sigma_x & \tau_{xy} & \tau_{xz} \\ \tau_{yx} & \sigma_y & \tau_{yz} \\ \tau_{zx} & \tau_{zy} & \sigma_z \end{bmatrix}$$

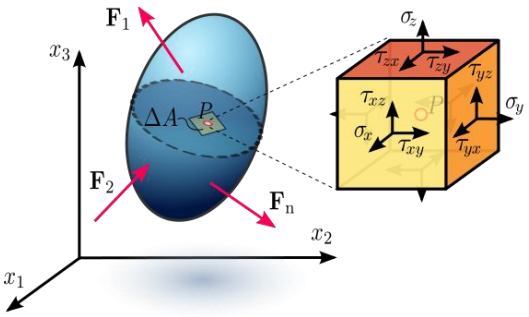

Figure 2. In a general case of loading, each element in the body is subjected to normal and shear stresses and is described by the Cauchy stress tensor [42].

The Eigen values of stress tensor are called principal stresses and the Eigen values of strain tensor are called principal strains. For the case of large deformations with non-linear behavior the finite strain theory is usually used to analyze the deformations.

$$S = JF^{-1}.\sigma.F^{-T}$$

where S is the second Piola-Kirchhoff stress tensor, F the deformation gradient tensor, $J = \det(F)$ the elastic volume ratio, and σ is the Cauchy stress tensor.

2.2. Mechanical theories of human soft tissues

The mechanical properties of human soft tissues are complicated and depend on age [16,67], subject, and even the location of force on a single subject [82]. Moreover, the human tissues are multi-layered, inhomogeneous, and anisotropic [28] meaning that their mechanical properties are not the same in all points and directions [11]. Biological soft tissues consist largely of water and exhibit both solid-like and fluid-like behavior which is called viscoelasticity. A viscoelastic material shows increasing strain under a constant load (creep), decreasing stress under a constant displacement (stress relaxation), and hysteresis under cyclic loading [44]. Human soft tissues are subjected to large deformations and their mechanical behavior is described by a non-linear relationship between stress and strain [28]. Hyper-elasticity provides a means of modelling the mechanical behavior of such materials [63,65]. A

hyper-elastic material is a rubber-like ideally elastic material for which the stress-strain relationship derives from a strain energy density function [65]. The stress-strain curve of hyper-elastic materials are similar to materials with fibers meaning that they show large strains for small stress when tangled fibers are aligned, but a large stress is required to achieve higher strains when the already aligned fibers are stretched [10,12]. Different hyper-elastic material models are constructed by specifying different strain energy density functions. Neo-Hookean [65] and Mooney-Rivlin [63] are two kinds of hyper-elastic materials which are extensively used for modelling of biological tissues. Due to the large deformability of soft tissues and based on the second Piola-Kirchhoff stress theory:

$$\sigma = J^{-1}F.S.F^{T}$$

Once the strain energy density is defined, the second Piola-Kirchhoff stress is computed as:

$$S = 2\frac{\partial W_s}{\partial C}$$

where W_s is the strain energy density function and C is the right Cauchy-Green deformation tensor defined by:

$$C = F^{T}.F$$

The Neo-Hookean model uses the following strain energy function:

$$\mathrm{W_s} = \frac{1}{2}\mu(\bar{\mathrm{I}}_1 - 3) + \frac{1}{2}\kappa(\mathrm{J}-1)^2$$

where $\bar{I}_1 = Tr(\bar{F}^T.\bar{F})$ is the first invariant of the Cauchy-Green deformation tensor, $J = \det(F)$ the elastic volume ratio, F the deformation gradient tensor, $\bar{F} = J^{-1/3}.F$ the isochoric component of deformation gradient tensor, and Tr trace of a matrix. Therefore, the Neo-Hookean model is defined by two constants: shear modulus (μ) which indicates the response to shearing strain, and bulk modulus (κ) which describes the resistance to normal compression.

2.3. Computational modelling of tissue biomechanics

Computational modelling of mechanical behavior of soft tissues is mostly based on finite element method (FEM). The finite element method is a highly advanced numerical approach

and a technique for discretization to establish an approximate solution of the partial differential equations governing physical systems [73]. It is mainly used where due to the physical complexities of the system a closed form solution is not feasible. The main factors causing complexity of the most of these systems are complex geometries, and two or three-dimensional boundary conditions. The principal concept of the finite element method is based on transforming the underlying differential equations describing the behavior of a physical system to a numerically solvable discrete formulation [73]. In the finite element method, the continuum domain of a model is divided (discretization) into a finite number of small non-overlapping subdomains with a simple geometry called (*finite*) *elements*. These elements can be found in tetrahedral or hexahedral forms and the boundaries of adjacent elements are connected by a number of points (*nodes*). The process of creating elements and nodes is called *mesh generation*. The problem solution is determined with regard to some field variables e.g. displacements, stress, and strain at the nodes. Unknown variation of these parameters at non-nodal points is estimated by a specific interpolation method (shape function) using the nodal points. Possible applications of finite element method are to evaluate the stress and strain fields, and deformations within the solid structures under any kind of external loading which makes it extremely beneficial in various research fields. The accuracy of finite element simulation is closely dependent on the mechanical parameters of the materials employed in modelling e.g. shear and bulk modulus in simulation of hyper-elastic materials. This accuracy is also strongly related to defining boundary conditions which can be found in various forms such as displacement, force, and pressure. In biomedical applications, construction of the geometry of the model and defining boundary conditions are of most challenging parts during finite element modelling. Human tissues are geometrically irregular and complex and in line the external loading conditions are not as simple as physical systems with regular geometry.

One reliable way for construction of the geometry of anatomical tissues is medical imaging techniques. The 3D data acquisition of the targeted soft and hard tissue is fundamentally performed using magnetic resonance imaging (MRI) or computer tomography (CT). Scanning provides a number of sequential 2D image slices of the structure. The scanning parameters should be adjusted in such a way to provide a clear anatomical delineation. To obtain the 3D geometry representation of the region, the 2D image slices are exported to a biomedical image processing program. The 3D segmentation of each tissue composing the structure and volumetric reconstruction are graphically performed to generate

the real 3D geometry of the model. Using a pre-processing tool, the surface or volumetric mesh is generated on the reconstructed model and is prepared to be exported into a finite element solver. The material properties and boundary conditions are determined in the solver. Since defining the accurate load boundary conditions is technically difficult, a feasible approach is to concentrate on the anatomical areas relevant to a specifically determined loading scenario. Alternatively, the boundary conditions can be extracted from the scanning data. In this case the scanning is performed at loading conditions and deformation of the tissue is obtained by manual segmentation of the slices and is prescribed to the model as displacement boundary conditions. In this project due to the heterogeneity of pressure distribution over the limb surface and lack of information about the various pressure values and their coordination on the skin, the three-dimensional map of indentations were extracted from the MRI data and applied to the finite element model to imitate the boundary conditions at different cuff compression intensities.

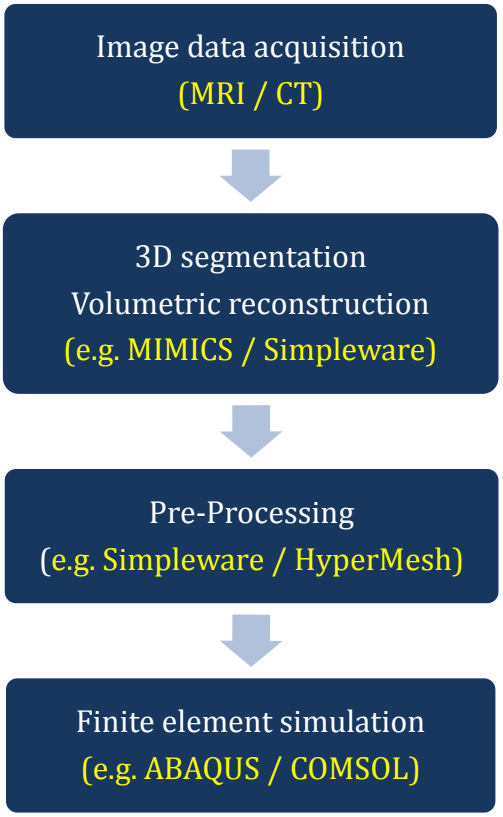

Figure 3. Procedure of finite element modelling of human tissues from imaging to simulation for stress/strain analysis.

Chapter 3

Methods and Materials

This chapter provides a concise overview of the experimental and computational methods employed in this project.

3.1. Deep-tissue stress and strain distribution

A finite element model has been developed (study I, II) to evaluate the magnitude and distribution of stress and strain in deep tissues during painful cuff algometry. Two experimental and six consecutively modelling phases were performed to develop such a simulation.

- Cuff algometry: Pain detection thresholds (PDT) and pain tolerance thresholds (PTT) to inflation of cuff were recorded by a computer-controlled cuff algometer. A 6-cm wide tourniquet air-cuff (VBM, Germany) was wrapped around the right lower leg of one subject at the level lower than the heads of the gastrocnemius muscle. The pressure increased with a rate of 1 kPa/s. The participant rated the pain intensity continuously during the pressure stimulation on an electronic Visual Analogue Scale (VAS). Zero and 10 cm on the VAS represented 'no pain' and 'maximal pain' and the cuff pressure at these two conditions was defined as PDT, and PTT value, respectively. The sampling rate of the electronic VAS was 10 Hz and the maximum pressure limit was 100 kPa. Based on PDT and PTT values three different stimulation intensities were defined: (1) mild stimulation (50% of the PDT intensity), (2) painful stimulation (PDT intensity), and (3) intense painful stimulation (5 cm on the VAS).

- MRI acquisition: Subsequently four MRI series including one condition without cuff pressure and three stimulated predefined conditions were performed on the right lower leg encompassing the 6 cm cuff width plus an additional 4.5 cm proximal and distal to the cuff, covering totally 15 cm of the limb. This was done using a 3T MRI scanner (Signa Optima 750, GE Healthcare, Milwaukee, WI, USA) based on a matrix of 512×512 pixels, 3 mm slice thickness, echo time (TE: 13.664 ms) and repetition time (TR: 660 ms) to provide a clear anatomical delineation (Fig. 4A). The number of slices was 17 for each condition.

- Indentation map: A manual segmentation was performed by MATLAB (Mathworks, USA) on total 68 MRI slices to specify the outline boundary of the model in each slice. The selected points on the outline boundary of the limb in each slice were connected together to make a contour (Fig. 4B). All 68 contours were unwrapped along the horizontal axis indicating the outline boundary as a function of angle (θ). By subtraction of the curves at stimulated conditions from non-stimulated condition the indentation curve was defined as a function of angle for each 17 slices at three stimulated conditions (Fig. 4C). An interpolation was performed on the indentation signals along the axial direction of the limb to obtain the 3D map of indentations around the limb in cylindrical coordination system and prescribe the finite element model.

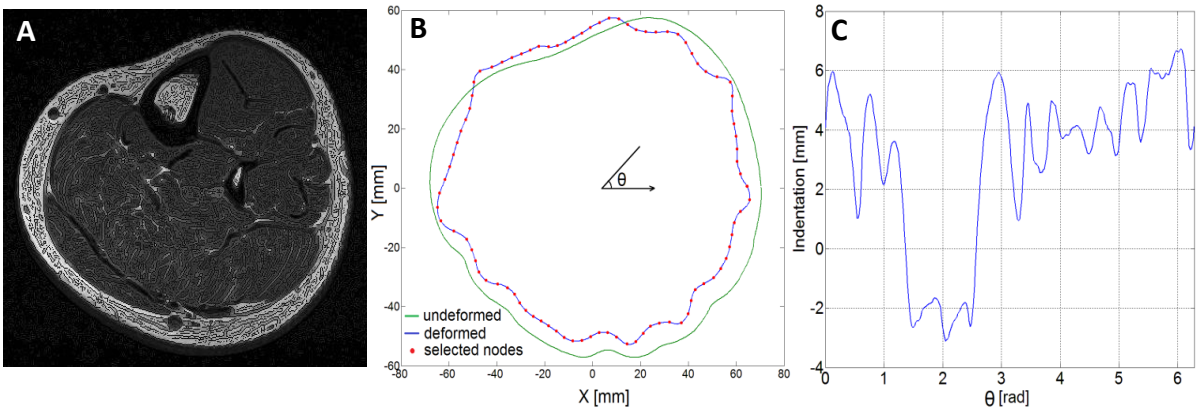

Figure 4. The process of deriving indentation map around the limb (A) a sample of transverse MRI scan of the lower leg located in the middle of cuff area (B) segmentation of the outline boundary in deformed and un-deformed conditions (C) indentation signal for one slice extracted by subtraction of deformed outline boundary from un-deformed boundary. Data are taken from study I, II.

- Volumetric reconstruction: The geometry of the model was based on four different anatomical structures including skin, subcutaneous adipose, muscle, and bones (Tibia and Fibula). 3D segmentation and image data visualization of each soft and hard tissue were performed by a professional biomedical image processing software (Simpleware, Exceter, UK). (Fig. 5A)

- Mesh generation: The finely detailed mesh was created within the same program based on 853,711 tetrahedral elements, 175,753 triangular elements, and 624,836 degrees of freedom (Fig. 5B). The entire volume of the model was 1,685,420 mm^3 divided into skin; 106,600 mm^3, subcutaneous adipose; 438,200 mm^3, muscles; 1,033,000 mm^3, tibia; 97,370 mm^3, and fibula 10,250 mm^3 (study I, II). Also, two surfaces were defined around

the bony structures representing the periosteal layers of hard tissue with 5,167 mm^2 and 14,660 mm^2 area for the fibula and tibia surfaces, respectively (study II).

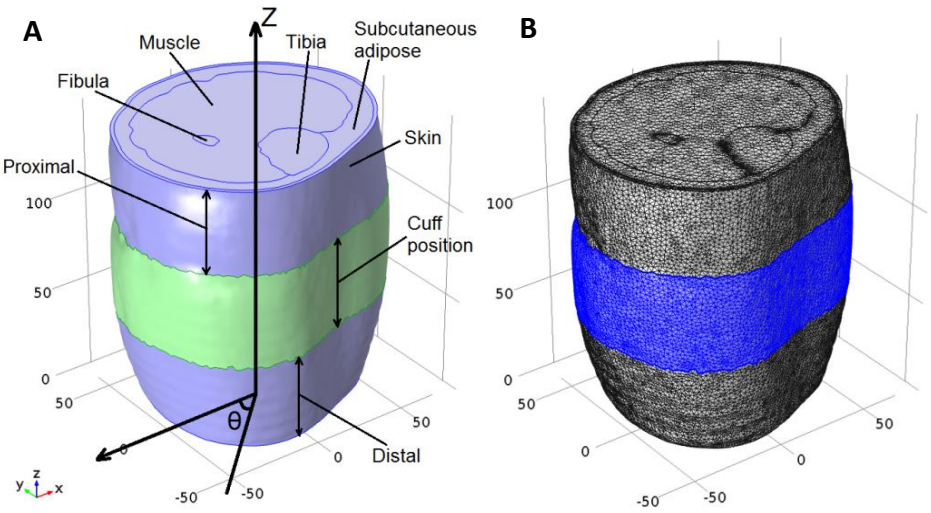

Figure 5. (A) Volumetric reconstruction of the scanned area including different anatomical structures, (B) 3D meshed model from z = 0 the distal side to z = 150 mm the proximal side used for finite element analysis. The blue area shows the cuff position. Data are taken from paper 2.

- Material parameters: The three-dimensional meshed model was exported to the finite element solver (COMSOL 4.3b Multiphysics, Sweden) to define the material properties and boundary conditions. The mechanical properties of the skin, subcutaneous adipose, and muscle were assumed to be non-linear, isotropic, and hyper-elastic with nearly incompressible version of the Neo-Hookean strain energy density function (study I, II). The bulk moduli (κ) and shear moduli (μ) of different soft tissues were adapted from a previous study [81]. The material constants used for the simulation of skin, subcutaneous adipose, and muscle tissue is represented in Table 1.

	Shear modulus, μ (kPa)	Bulk modulus, κ (kPa)
Skin	200	3000
Subcutaneous adipose	1	36
Muscle	7.44	116

Table 1. The material parameters of Heo-Hookean model used for finite element simulation of soft tissues, based on data from Tran et al. (2007).

The model included two long bones (Tibia and Fibula) which were assumed to be rigid meaning that they did not show any deformation under the loading conditions (study

I), whereas to investigate the effects of cuff compression on the periosteal layers on the external surface of the hard tissues, the bones were assumed to be linear elastic materials (study II). This kind of material was defined based on 7300 MPa as Young's modulus and 0.3 as Poisson's ratio [13].

- Boundary conditions: All nodes of three soft tissue layers were left free to have displacement in space in all directions (study I, II). The boundary condition of the nodes of the bony structures was defined as fixed constraint meaning that they did not have any displacement in the space during the simulation (study I). These nodes were only constraint in axial direction of the model (study II) meaning that they were left free to have relative or absolute displacement in the transverse plane (xy-plane) but their displacement in axial direction (z-axis) were zero. The extracted 3D indentation maps were converted from cylindrical coordination system to the Cartesian system and were applied to the external surface of the model as prescribed displacements simulating the external boundary conditions at mild, painful, and intense painful cuff compression intensities.

- Simulation: The indentation intensities incrementally increased by 0.5 mm step during the simulation progress to prevent the convergence problem which is very common in running the hyper-elastic models. Also, due to the high non-linearity of this model, a conservative and robust constant-predictor approach was used during the solution. This technique is based on the use of the final condition of one step of the simulation as the initial condition to the following step. Finally, when the prescribed displacement boundary conditions reached the actual magnitudes, the running process was stopped and the solution was completed. The indentation fields, stress, and strain distributions of each layer of the soft tissues were extracted from the solved model (study I). The pattern of stress and strain on the external surface of bony structures and on the muscle surface were also obtained (study II).

3.2. Spatial pressure distribution on limb surface

The experimental and analytical approaches were employed (study III) to characterize the interface pressure distribution between the cuff and limb during painful cuff algometry.

- Cuff pressure algometry**:** Two kinds of tourniquet cuffs were used in this study. An air-cuff (VBM, Germany) and a water-filled cuff (Nocitech, Denmark) were separately mounted on the right leg of twelve subjects (six females; age range: 23-33 years; mean age: 29; lower leg circumference: 31-36 cm; BMI: 18.8-25.5) lower than the heads of the gastrocnemius muscle, with the cuff centered at the level with the maximum leg circumference. The air-cuff was a conventional tourniquet chamber while the water-cuff had an inner cylindrical water-filled chamber and an outer air-inflated chamber non-mixing with water. The cuffs were inflated by a ramp function with the slope of 1 kPa/s provided by a computer-controlled air compressor. The participants rated their pain intensity using the VAS system where the PDT and PTT values were recorded. The measurement was performed three times with a 2 min resting interval and the mean of pressure values was calculated as the final values of PDT and PTT for each subject. This procedure was separately conducted using two kinds of cuffs.

- Measurement of interface pressure: A flexible and elastic sensor mat type S2119 (novel GmbH, Munich, Germany) containing 32×16 pressure sensors was used to record the interface pressure. The size of each embedded sensor was 10×10 mm^2 which was able to measure the pressure values up to 400 kPa. The pressure mat was placed between the cuff and the skin where the interface pressure was recorded at 32×16 coordinates inside and outside the cuff area during the ramp inflation until the previously recorded pressure tolerance level. The minor interface pressure values before the inflation of cuff was calibrated to zero to prevent the effects of this passive pressure on the real values during the cuff inflation.

- Data analysis: The mean interface pressure was calculated in the rectangular area under the cuff position over the cuff stimulations. The pressure distribution frames representing the pattern of interface pressure at different cuff stimulation intensities (10, 20, 30, 40 kPa) and also at pain detection and pain tolerance conditions were extracted for further analysis. In order to compare the *variability* of the pressure distribution generated by air-cuff and water-cuff, the standard deviation of the interface pressure distribution was calculated at the mentioned intensities. Lower standard deviation shows the reduced variability of pressure distribution and hence indicates the ability of cuff to stimulate lager areas around the limb with the pressure values near the mean interface pressure. To assess the *homogeneity* of interface pressure the entropy of the matrix of interface pressure

distribution was calculated. The entropy is a non-negative scalar value showing the uniformity of a distribution X and is calculated by the following formula [6]:

$$H(X) = -\sum_{i} p_i * \log(p_i)$$

where p_i are the probability values composing the distribution X. Lower amount of entropy indicates the more homogeneity of that distribution. In this study the histogram of the non-zero cells of the matrix of interface pressure was derived at the specified cuff pressure intensities. Using this histogram which roughly estimates the probability density function of interface pressure distribution the p_i values were extracted and the entropy values were calculated for the all subjects at four consecutively pressure intensities, pain detection, and pain tolerance conditions.

Chapter 4

Results

This chapter presents a concise summary of the findings in this Ph.D. project. For details, the reader is referred to the full length articles.

4.1. Tissue mechanics during painful cuff stimulation

Below, results regarding the mechanical influences of cuff compressions on deep somatic tissues (study I, II) are presented.

4.1.1. Indentation maps

Based on pain detection and pain tolerance thresholds (Mean ± SD), the 9.7 ± 1.4 kPa, 19.4 ± 2.9 kPa, and 30.2 ± 3.8 kPa were used for provocation of mild, painful, and intense painful stimulations, respectively. The three-dimensional map of indentations in cylindrical coordinate system applied to the finite element model (study I, II) is represented in Fig. 6.

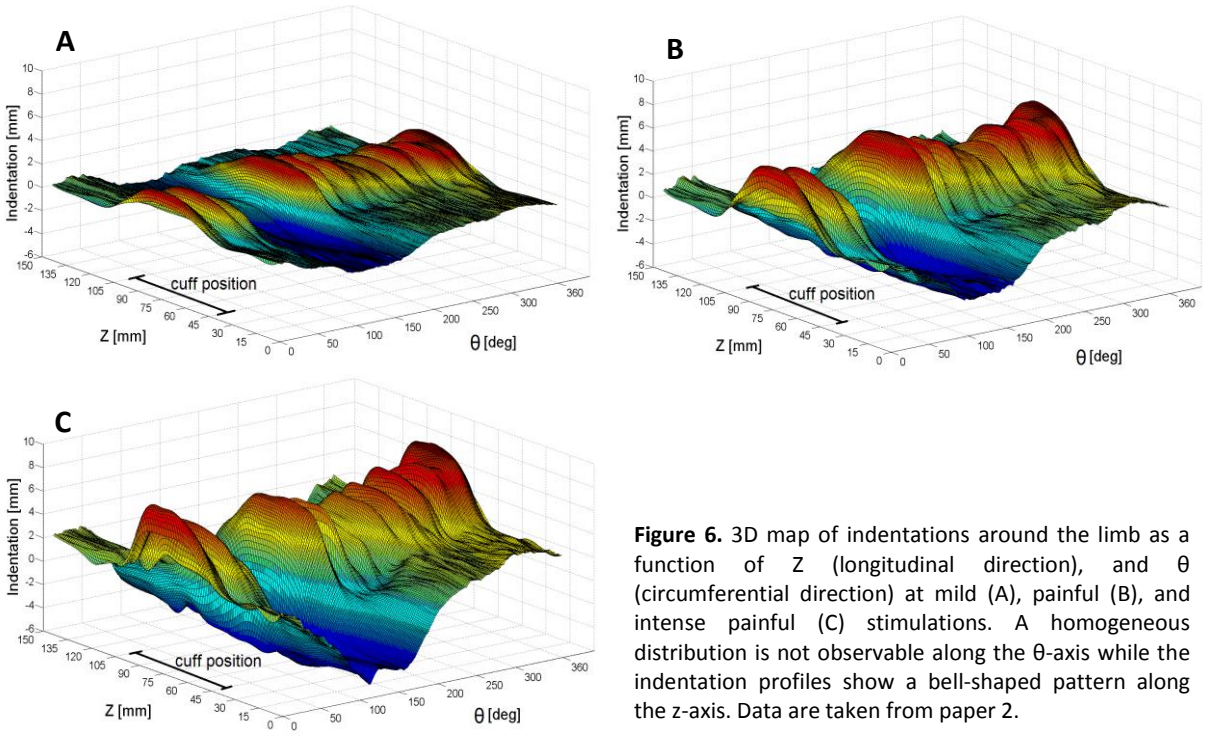

Figure 6. 3D map of indentations around the limb as a function of Z (longitudinal direction), and θ (circumferential direction) at mild (A), painful (B), and intense painful (C) stimulations. A homogeneous distribution is not observable along the θ-axis while the indentation profiles show a bell-shaped pattern along the z-axis. Data are taken from paper 2.

Generally, the indentation map showed a bell-shaped form along the z-axis peaking in the cuff position area; however, a regular pattern of indentation was not observed along the θ-axis. Interestingly, the indentation profiles along the θ-axis demonstrated that the circumferential areas around the tibia bone site (θ = 81° to 158°; Fig. 6) were subjected to the negative indentation toward the outside of the model whereas the compressive loading was applied to the limb.

4.1.2. Tissue deformations

Based on the FE simulations, the deformation pattern during the increasing trend of cuff compression intensity is shown in Fig. 7 for the mid-transverse planes located distally to the cuff (A, B, C), proximally to the cuff (G, H, I), and in cuff position (D, E, F) (study I).

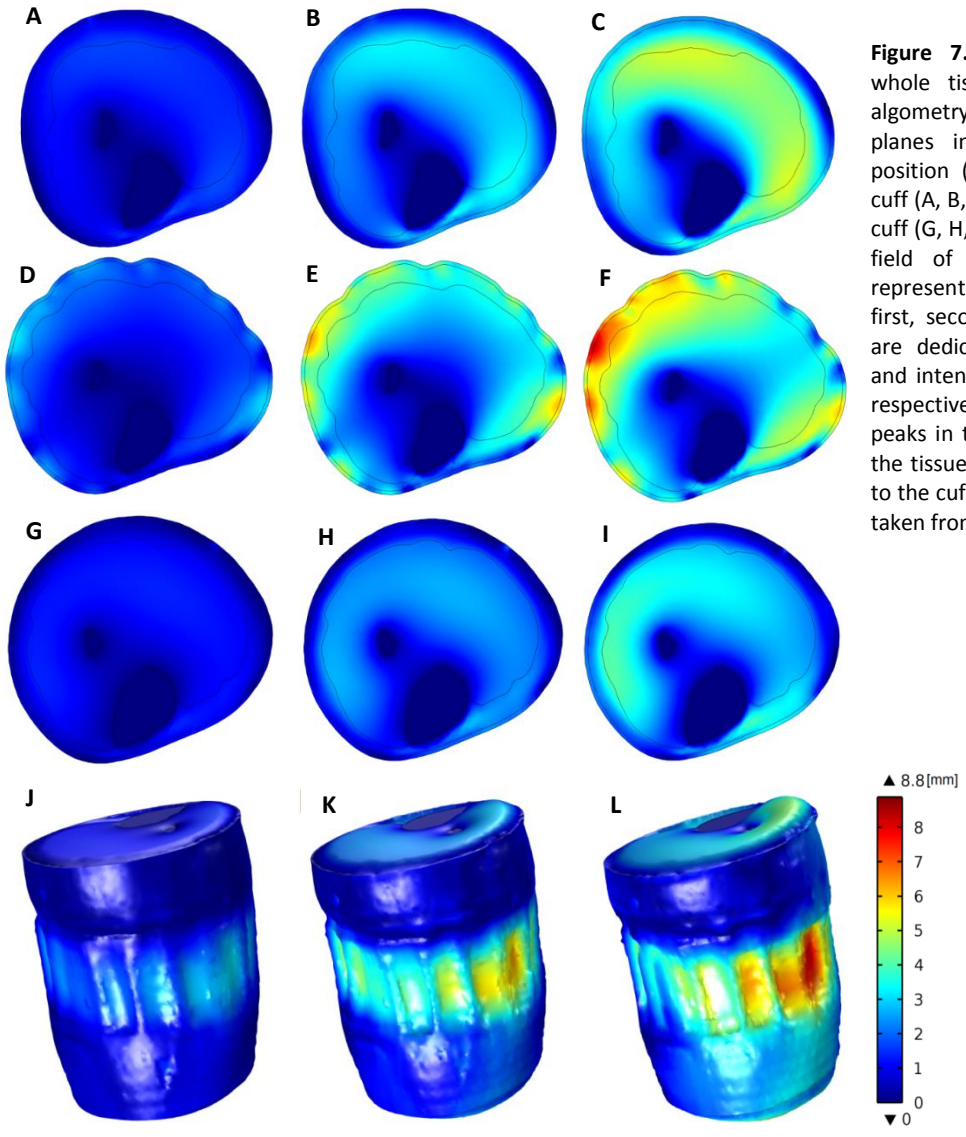

Figure 7. Deformation of the whole tissues during the cuff algometry in the transverse planes in the center of cuff position (D, E, F), distal to the cuff (A, B, C), and proximal to the cuff (G, H, I). The 3D deformation field of the entire model is represented in the last row. The first, second, and third columns are dedicated to mild, painful, and intense painful stimulations, respectively. The deformation peaks in the cuff position where the tissues are directly subjected to the cuff compression. Data are taken from paper 1.

The FE simulations showed that the intensity of deformation was dependent on the axial position. As expected, the tissues inside the cuff area were more stimulated compared to the tissues outside the cuff area. The three-dimensional analysis illustrated that the maximum deformation happened approximately at the height which is located in the center of the cuff and under the direct pressure of cuff bladders (Fig. 7J, K, L). Anatomically, this location is at the peroneal muscle site in the lateral compartment of the leg (Fig. 7F, L). Distally and proximally to the cuff the deformation peaked at two opposite site of the limb (Fig. 7C, I). Distal to the cuff the tissues of gastrocnemius and soleus muscle showed higher deformation (Fig. 7B, C) while proximal to the cuff the areas around the tibialis anterior muscle were subjected to the higher deformation (Fig. 7H, I).

4.1.3. Nodal displacement field

The two-dimensional nodal displacement field for the transverse plane located at the center of cuff position at three cuff compression intensities and three-dimensional displacement field for intense painful condition extracted from FE simulation are represented in Fig.8 (study I). Each vector indicated the magnitude and direction of the displacement of each node composing the FE model. The indentation vectors represented that the tissues outside the cuff area were more subjected to the axial displacement while the tissues beneath the cuff were subjected to the radial displacement. The two-dimensional figures also showed that those radial displacements were diverted from the radial direction in the areas around the

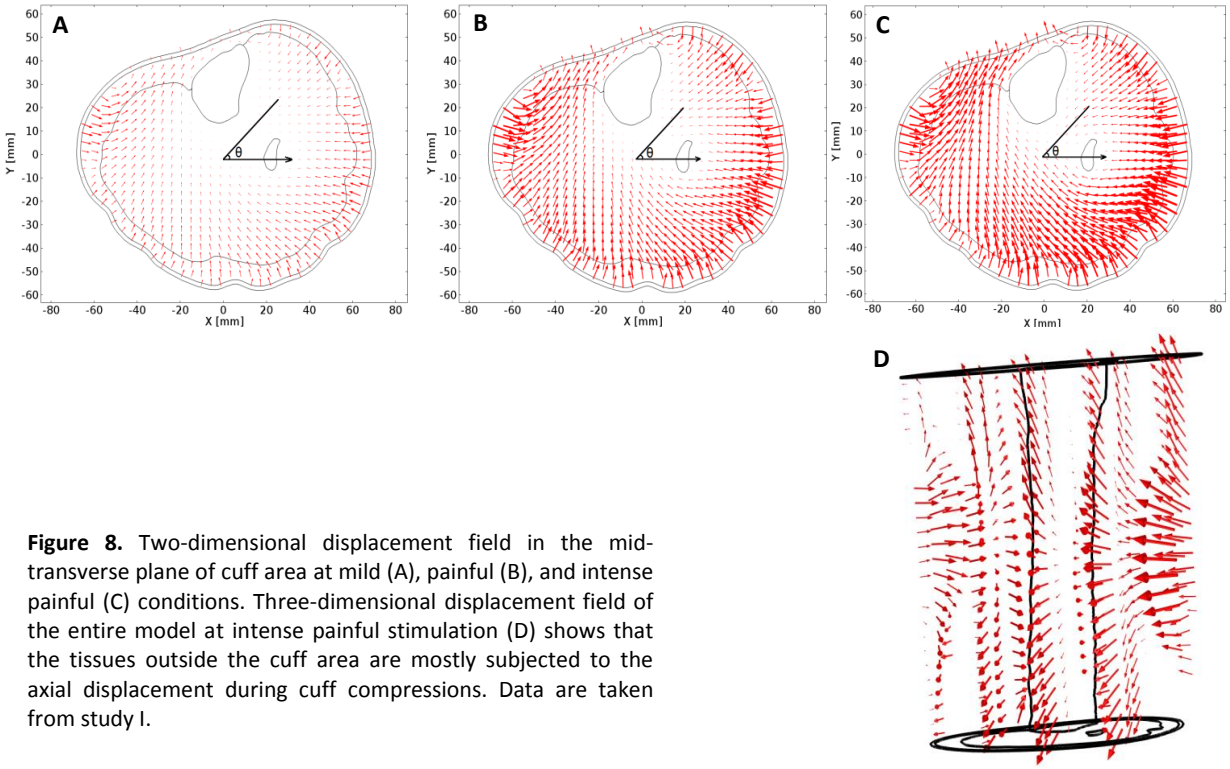

Figure 8. Two-dimensional displacement field in the mid-transverse plane of cuff area at mild (A), painful (B), and intense painful (C) conditions. Three-dimensional displacement field of the entire model at intense painful stimulation (D) shows that the tissues outside the cuff area are mostly subjected to the axial displacement during cuff compressions. Data are taken from study I.

4.1.4. Stress distribution of muscle tissue

The stress in the transverse plane at the center of the cuff area (Fig. 9D, E, F), distal (Fig. 9A, B, C), and proximal (Fig. 9G, H, I) to the cuff showed an increasing pattern from the mild to intense painful stimulation (study I). Distally and proximally to the cuff, the stress was concentrated around the bones whereas inside the cuff area the stress was more extensively distributed over the muscle tissue. The three-dimensional model confirmed that the regions with stress concentration were located around the edge of the bones in all three stimulation intensities (Fig. 9J, K, L). Moreover, during the enhancement of the cuff compression intensity, the areas with stress concentration were observed in the cuff position; in particular along the axial direction the stress had an increasing pattern toward the center of the cuff area

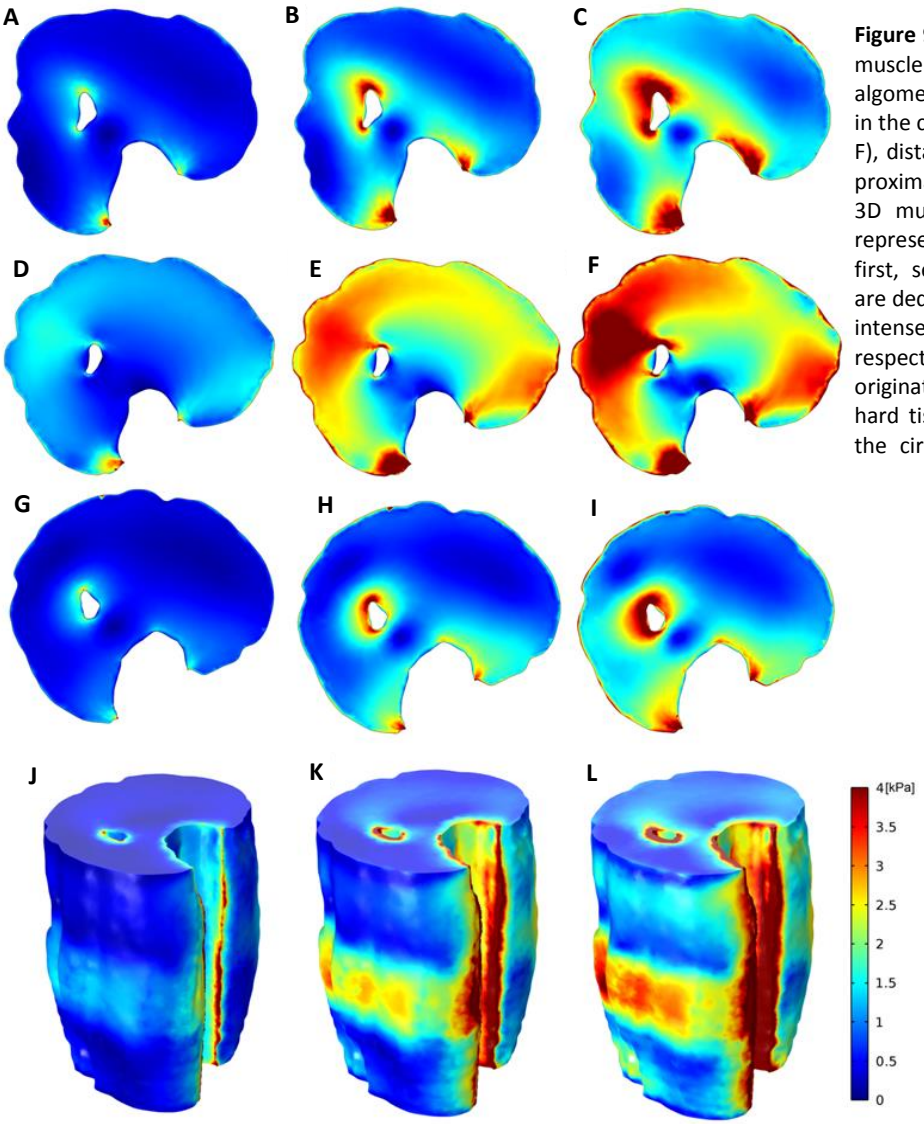

Figure 9. Stress distribution of the muscle tissue during cuff algometry in the transverse plane in the center of cuff position (D, E, F), distal to the cuff (A, B, C), and proximal to the cuff (G, H, I). The 3D muscle stress distribution is represented in the last row. The first, second, and third columns are dedicated to mild, painful, and intense painful stimulations, respectively. The stress pattern originates from the edge of the hard tissues and is distributed to the circumferential areas of the

4.1.5. Surface stress distribution

The finite element simulations demonstrated that the stress distribution on muscle (Fig. 10A, B, C), tibia (Fig. 10D, E, F), and fibula (Fig. 10G, H, I) surfaces increased from the mild to intense painful stimulations (study II). On muscle surface the stress is mainly focused in the cuff position region. For the tibia surface the areas with stress concentration was in correspondence with the lower parts of the cuff position. However, for the fibula surface the stress was more distributed along the bone and not concentrated in a specific location.

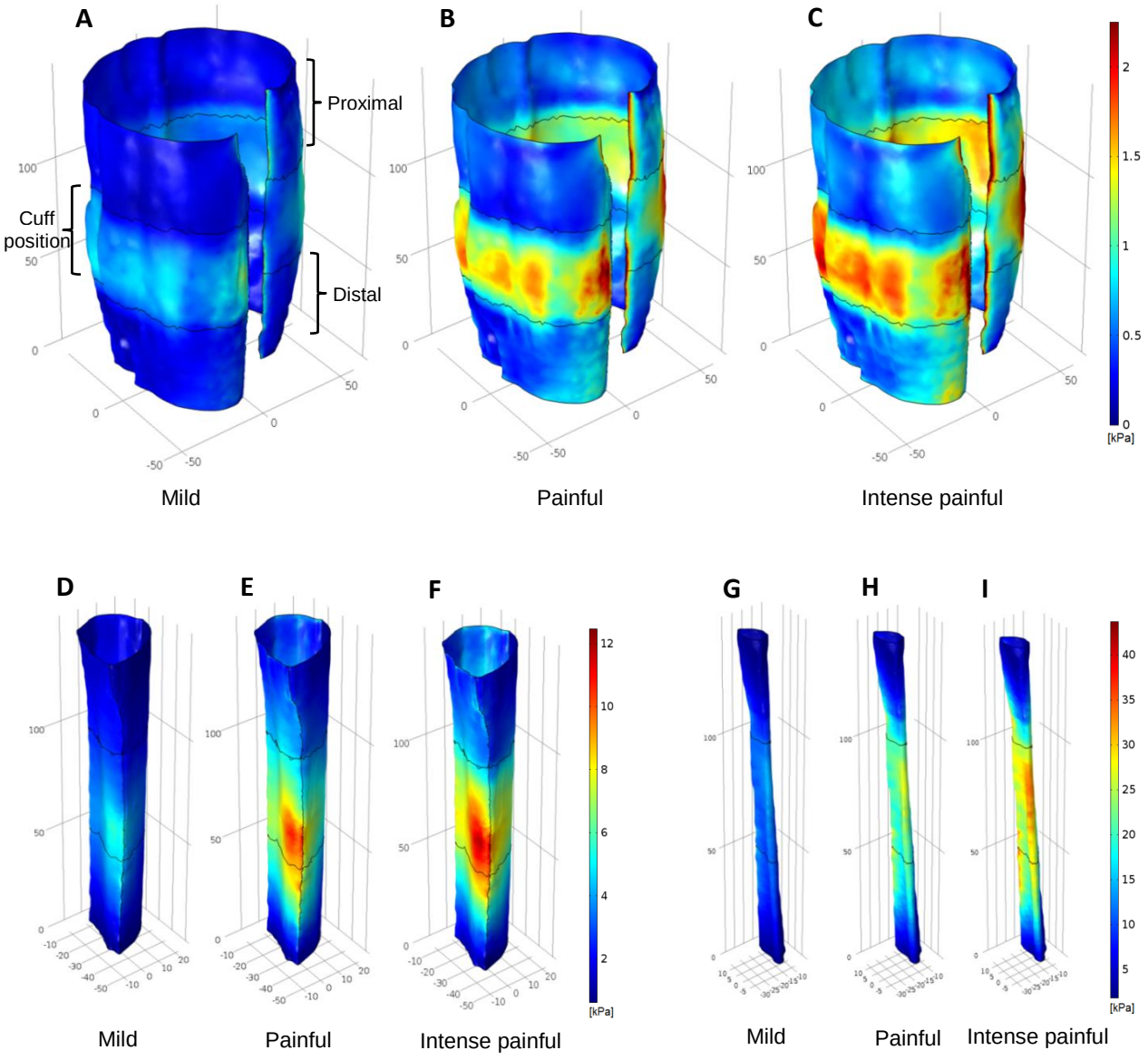

Figure 10. The stress distribution on muscle surface (A, B, C), tibia surface (D, E, F), and fibula surface (G, H, I) at different cuff compression intensities. The stress in mainly focused in cuff position area and increases from mild to intense painful stimulations. Data are taken from paper 2.

4.1.6. Strain distribution of muscle tissue

The strain pattern increased from mild to intense painful stimulation in the transverse plane at the center of cuff position (Fig. 11D, E, F), distal (Fig. 11A, B, C), and proximal to the cuff (Fig. 6G, H, I) (study I). The figures of transverse planes showed areas with strain concentration around the bony structures occurring mostly outside the cuff position. Moreover, the muscle tissues were subjected to the higher amount of strain inside the cuff area compared with the muscle tissue outside the cuff position. The three-dimensional simulations also confirmed that the areas with strain concentration could be found around the edge of hard tissues whereas on the muscle surface the strain was irregularly distributed along the axial direction (Fig. 11J, K, L).

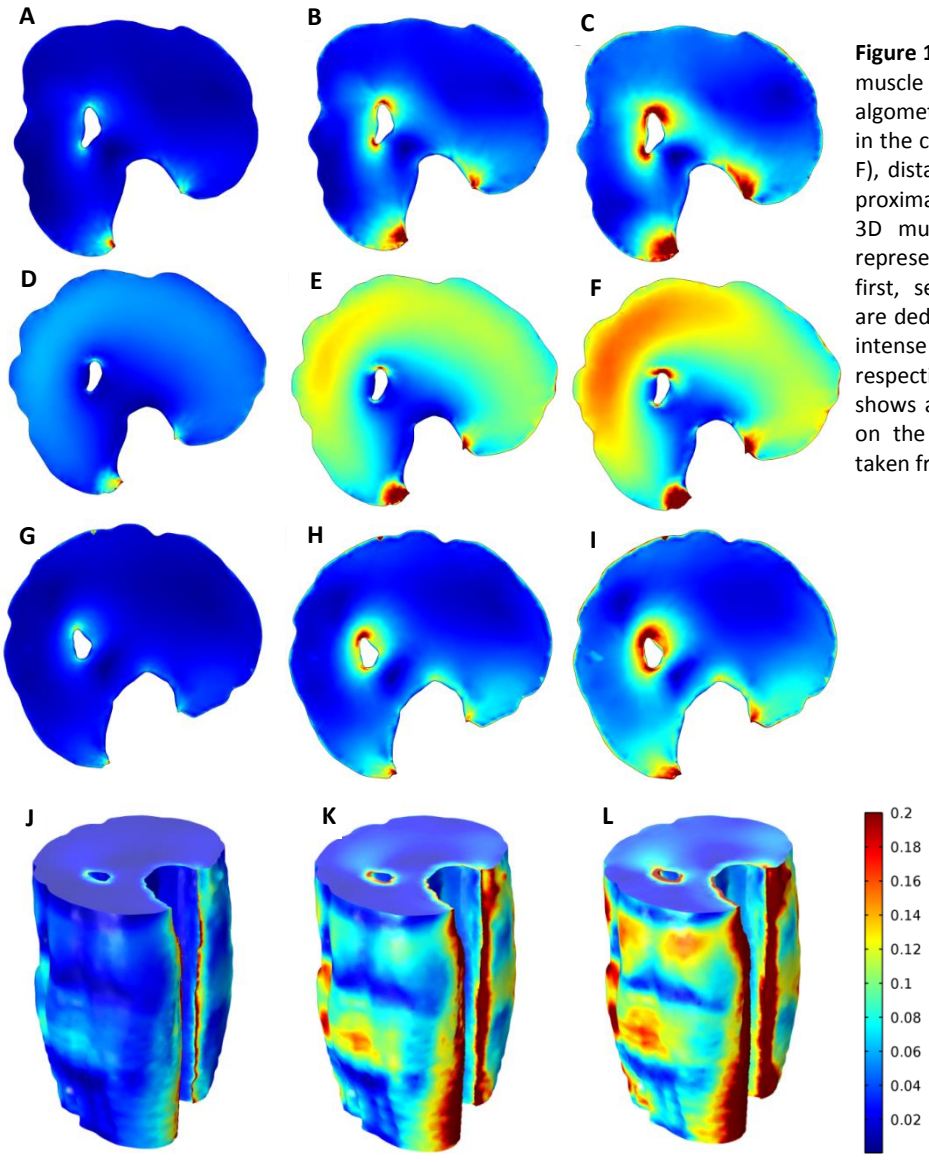

Figure 11. Strain distribution of the muscle tissue during cuff algometry in the transverse plane in the center of cuff position (D, E, F), distal to the cuff (A, B, C), and proximal to the cuff (G, H, I). The 3D muscle strain distribution is represented in the last row. The first, second, and third columns are dedicated to mild, painful, and intense painful stimulations, respectively. The strain pattern shows an intermittent distribution on the muscle surface. Data are taken from paper 1.

4.1.7. Surface strain distribution

The strain had an increasing trend on the muscle (Fig. 12A, B, C), tibia (Fig. 12D, E, F) and fibula (Fig. 12G, H, I) surfaces when the cuff compression intensity increased from mild to intense painful stimulation (study II). The strain on muscle surface was not concentrated in a specific part and was more distributed compared with the stress on this surface. On the tibia surface the strain was mostly concentrated on the side of tibia which is directly attached to subcutaneous adipose and is not covered by muscle tissue. For the fibula surface the areas with greater strain were not observed in the cuff area and were mostly distributed outside the cuff area.

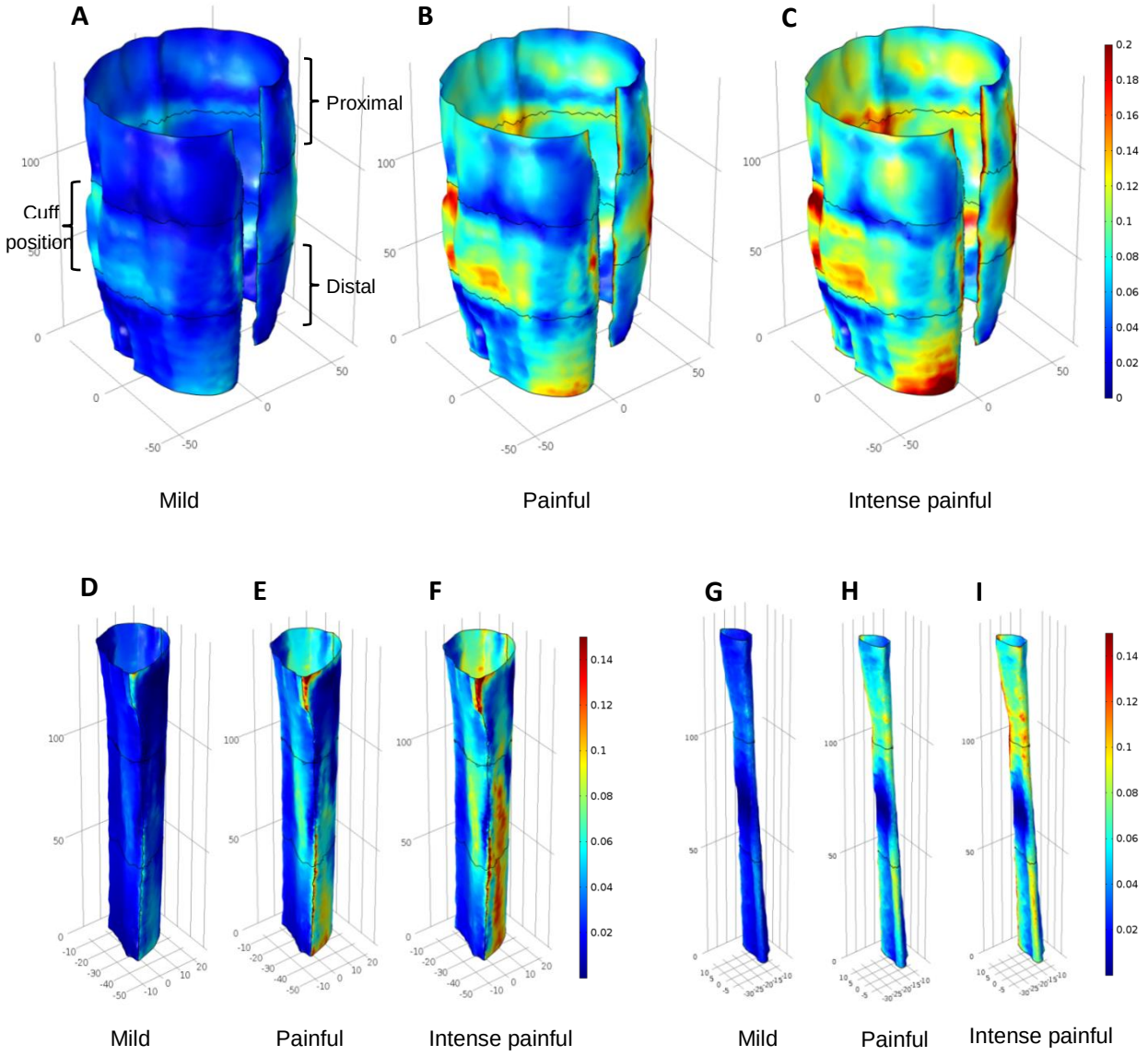

Figure 12. The strain distribution on muscle surface (A, B, C), tibia surface (D, E, F), and fibula surface (G, H, I) at different cuff compression intensities. The increasing pattern of strain is observable from mild to intense painful conditions. The strain shows a more widespread distribution rather than stress. Data are taken from paper 2.

4.1.8. Quantitative analysis of stress and strain

The data of stress comparison among different volumetric tissues (study I) demonstrated that in all stimulation intensities the skin compartment was subjected to the highest amount of stress while the stress value dramatically decreased in subcutaneous adipose and muscle compartments (Fig. 13A). For instance, at painful threshold condition the mean stress of the skin layer was 52.4 kPa whereas the mean stress in subcutaneous adipose and muscle tissue was 1.2% and 2.9% of the mean stress in skin tissue, respectively (Fig. 13A). Interestingly, the mean strain peaked in subcutaneous adipose and decreased in other tissues (Fig. 13B). At painful threshold intensity the mean strain of the subcutaneous adipose layer was 0.027 while the mean strain of skin and muscle tissue was 69.0% and 55.1% of the mean strain in subcutaneous adipose layer, respectively (Fig. 13B).

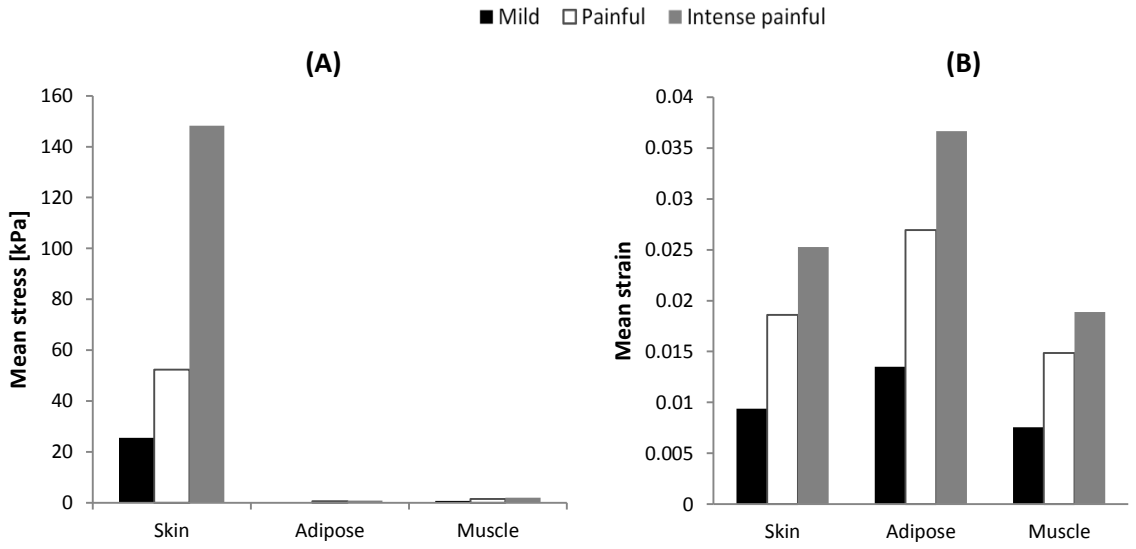

Figure 13. The mean stress (A) and strain values (B) in skin, subcutaneous adipose, and muscle tissue at different cuff compression intensities. The skin is subjected to the greatest value of stress while subcutaneous adipose is subjected to the greatest amount of strain during cuff algometry. Data are taken from paper 1.

The data of stress comparison among innervated layers (study II) showed that the tibia and fibula surfaces were subjected to greater values of mean stress in the all parts inside and outside of the cuff area compared to the muscle surface (Fig. 14A). For instance, the mean stress at painful condition in cuff-position area of tibia and fibula surfaces was 4.6 and 14.8 times greater than the same part of the muscle surface, respectively (Fig. 14A). However, the mean strain peaked on the muscle surface and decreased on the tibia and fibula surfaces inside and outside the cuff position and also at all three stimulation intensities (Fig. 14B). At painful

condition, the mean strain on the tibia and fibula surfaces in the cuff area was 36.5% and 32.9% of the mean strain in the same part of the muscle surface, respectively (Fig. 14B).

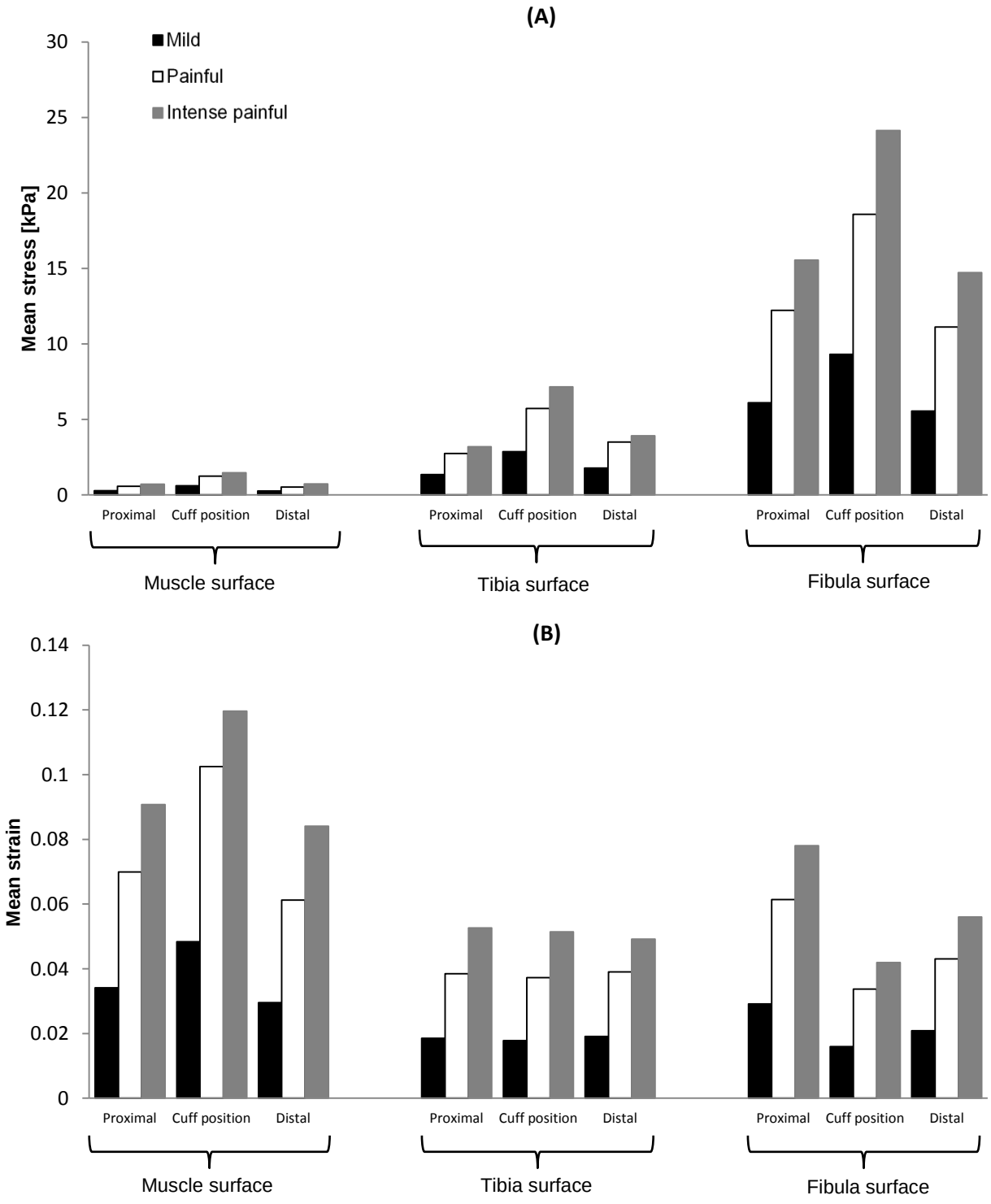

Figure 14. The mean stress (A) and strain values (B) on innervated layers including muscle, tibia, and fibula surfaces at different cuff compression intensities. Generally, the bony surfaces are subjected to the higher amount of stress whereas the muscle surface is subjected to the greater amount of strain during cuff algometry. Data are taken from paper 2.

4.2. Interface pressure behavior

Below, results regarding the characteristics of interface pressure distribution between the cuff and limb and the effects of using a liquid medium on this distribution are presented (study III).

4.2.1. Painful cuff algometry and interface pressure

During the air-cuff algometry the mean interface pressure across the entire stimulation area was not significantly different from the inflating cuff pressure at the PDT and PTT conditions. However, there was a significant decline in the mean interface pressure compared with the cuff pressure at both the PDT (20.8±5.8 kPa vs 28.0±10.1 kPa; $P < 0.002$) and PTT (41.3±10.0 kPa vs 72.0±11.6 kPa; $P < 0.002$) conditions during the water-cuff algometry. The mean values of cuff pressure and interface pressure for the all subjects at pain detection and pain tolerance conditions are shown in Fig. 15 (study III).

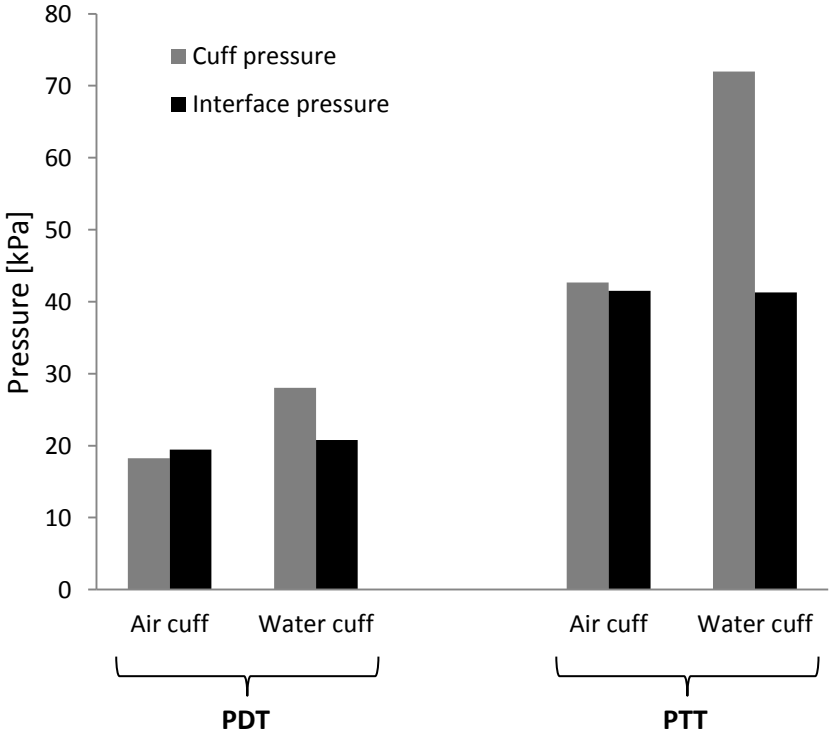

Figure 15. The mean values of cuff and interface pressure calculated for all subjects at PDT and PTT conditions during air-cuff and water-cuff algometry. The interface pressure is the mean value across the entire interface surface. The deviation of interface pressure from inflating cuff pressure was significant during water-cuff algometry. Data are taken from study III.

4.2.2. Interface pressure distribution

The distribution of interface pressure around the limb for one of the subjects at 30 kPa cuff pressure stimulation is represented in Fig. 16 during the air-cuff and water-cuff algometry (study III). Generally, at each specific point on θ-axis (circumferential direction) the pattern of interface pressure showed approximately a bell-shaped form along the z-axis (axial direction) meaning that the pressure values decreased close to the cuff edges and increased at the central regions of cuff. However, a specific pattern of pressure distribution was not observed along the circumferential direction during the air and water cuff algometry.

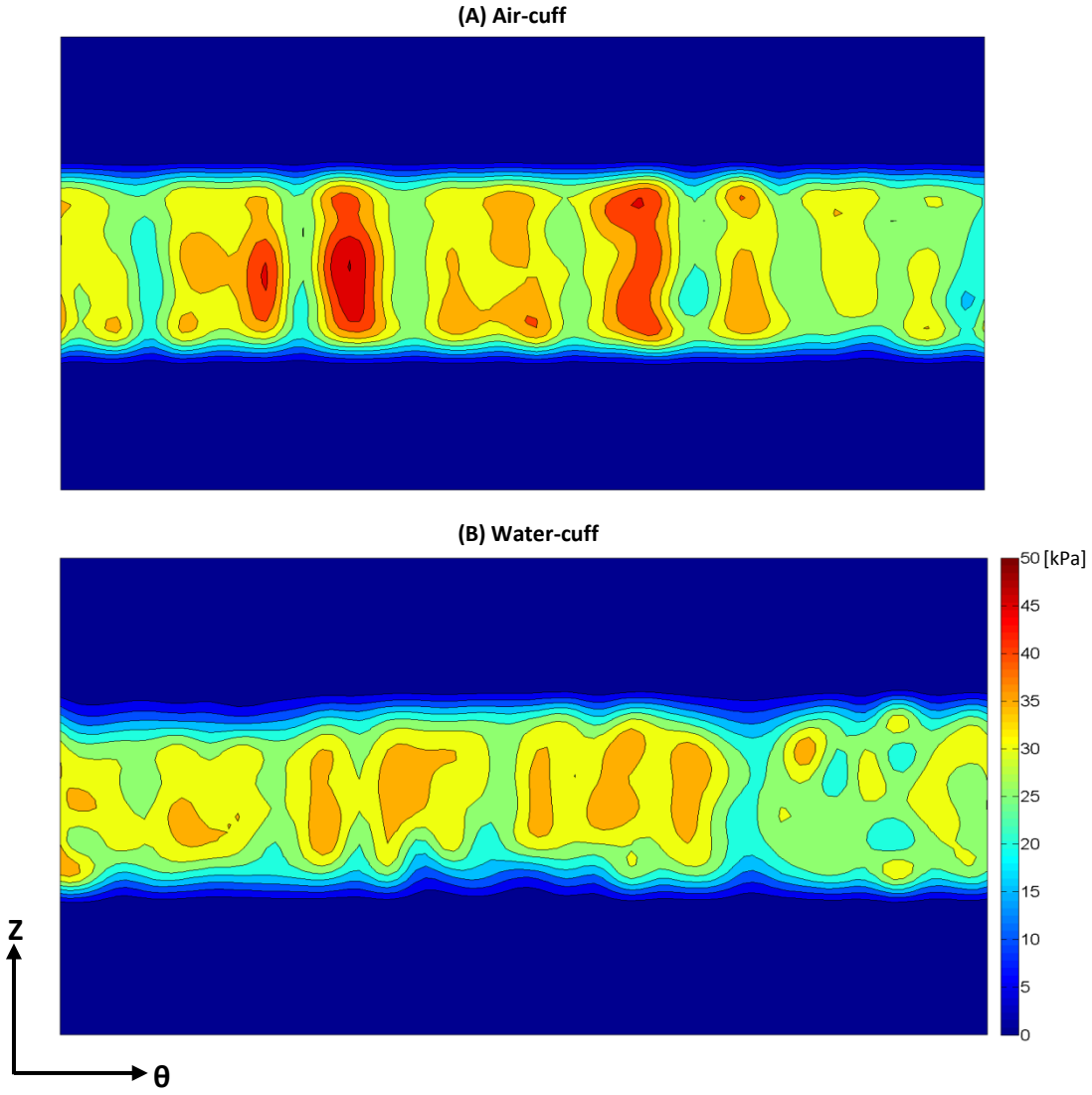

Figure 16. Two-dimensional distribution of interface pressure between the cuff and limb for one of the subjects as a function of Z (axial direction) and θ (circumferential direction) at 30 kPa cuff pressure using the air-cuff (A) and water-cuff (B). The pressure values peak at the central region of cuff area and decrease close to the edges of the cuff. A regular pattern is not observable along the θ-axis. Data are taken from study III.

The mean standard deviation of interface pressure distribution for all subjects as a function of cuff inflating pressure is represented in Fig. 17A (study III). In both types of the cuffs the standard deviation of interface pressure distribution had an increasing trend when the cuff pressure was increasing ($P < 0.001$). There was a significant difference between the standard deviation of water-cuff and air-cuff ($P < 0.027$). Moreover, a significant interaction between the cuff type and stimulation intensity was observed ($P < 0.036$). For pressure values more than 10 kPa the standard deviation of interface pressure distribution generated by the water-cuff was significantly lower than the air-cuff (Fig. 17A; $P < 0.04$).

The mean entropy of interface pressure distribution for all subjects during the cuff inflation increased over stimulation intensities (Fig. 17B; $P < 0.001$). Also, the entropy of water-cuff pressure distribution was significantly lower than the air-cuff during the stimulation intensities ($P < 0.032$).

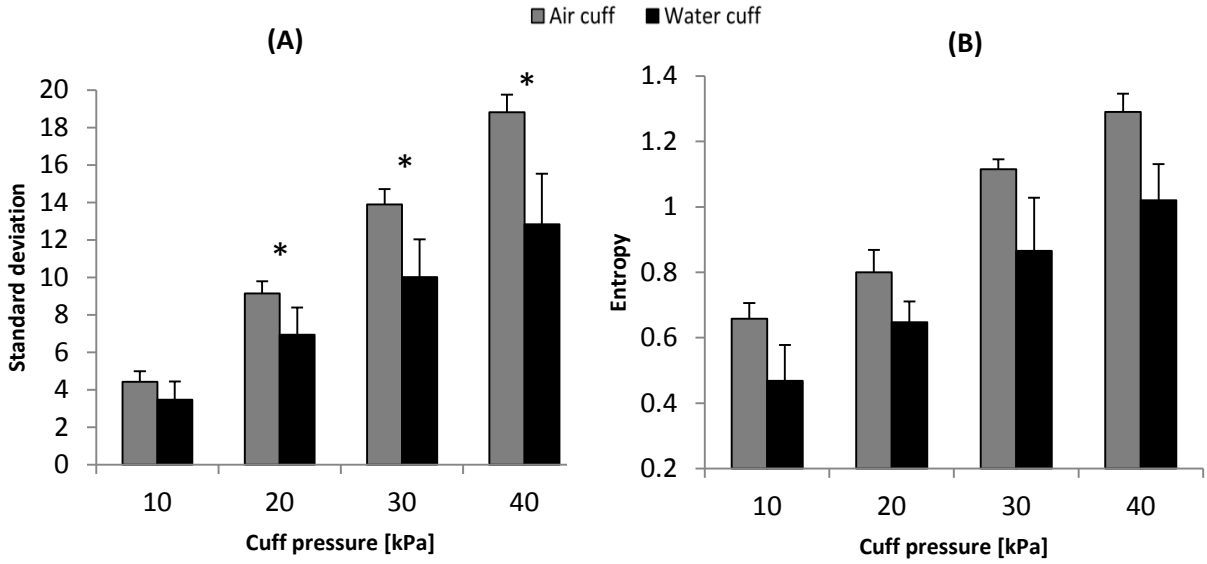

Figure 17. Mean (± SD, N=12) standard deviation (A), and entropy (B) of interface pressure distribution over cuff pressure intensities. The standard deviation and entropy showed an increasing trend when the cuff compression increased (P<0.001). The standard deviation of interface pressure distribution generated by water-cuff was lower than the air-cuff (*: P<0.05). The entropy of interface pressure distribution for the water –cuff was significantly lower than air-cuff over the stimulation intensities (P<0.032). Data are taken from study III.

Chapter 5

Discussion

The overall goal of this project was to provide a new insight into the intrinsic and extrinsic factors which are involved in mechanically induced pain during cuff pressure algometry. To study the intrinsic factors i.e. stress and strain distribution in different tissues (study I, II), a computational finite element model of the lower leg was developed. In line, to investigate the extrinsic factors i.e. behavior of interface pressure (study III), the spatial distribution of this pressure generated by two types of cuff algometry systems was characterized. The main findings of these studies were: (1) Tissue indentations is heterogeneously distributed during air-cuff pressure stimulations (study I, II); (2) Cuff algometry is able to extensively stimulate deep-tissue nociceptors by un-localized distribution of stress and strain (study I); (3) Cuff algometry is more capable to stimulate the nociceptors around the bony structures in terms of stress rather than strain compared with the more superficial muscle structures (study II); (4) Cuff systems with a liquid medium cause a significant decline in the amount of interface pressure exerted on the limb surface (study III); (5) Water-cuff systems generate a more homogeneous pressure distribution around the limb compared with the air-cuff systems (study III).

5.1. Three-dimensional map of indentations during cuff stimulations (study I, II)

Biomechanically the limb is not a uniform system and its geometry is irregular. Therefore, a homogeneous pattern of indentation is not observable along the longitudinal axis (z) and phase angle (θ). The indentation values reach the highest magnitude in cuff position area along the z-axis. Inside the cuff position the pattern of indentation is not flat and shows a bell-shaped profile along the z-axis. This means that the highest value of indentation is observed at the center of cuff position along the axial direction and the indentation values decrease close to the cuff edges. The variations of indentation along the z-axis is in correspondence with the pressure curve which has been previously demonstrated that has a parabolic form peaking under the mid-point of the cuff and reaching the smallest value at the proximal and distal edges of the cuff [31]. The behavior of indentation maps along the θ-axis is not regular. This is highly associated with the different anatomical tissues composing the limb while moving

circumferentially. Also, it has been acknowledged that there are variations in response to loading among different material components inside the calf [64].The negative indentation in the anterior site of the tibia is related to the inflation of cuff between the leg and bench causing an upward movement in the whole limb during the scanning. Due to the compressibility of soft tissues, this movement is not observable in these tissues. Rigidity of bony structures and the minimal thickness of soft tissues in the anterior site of the tibia are two important factors that explain the inverse indentation in this region.

The three-dimensional nodal displacement revealed different kinds of mechanical loadings which are generated in the limb during cuff compressions. Based on this the cuff pressure has compressive effects on the muscle tissues inside the cuff area and tension effects on the tissues outside the cuff area. Inside the cuff area and around the gastrocnemius and soleus muscles, the diversion of nodal displacements from the radial direction confirms the torsion effect of cuff compression on these muscles. Thus, it may be hypothesized that the cuff inflation has several biomechanical loading influences including radial compression, torsion, and axial tension. The compressive loading in the cuff position causes reduction of calf cross-sectional area which has been studied for the transverse plane at the center of cuff area [64]. However, the information on the biomechanical effects of other types of loading during cuff algometry is lacking.

5.2. Deep-tissue influences of cuff stimulations (study I)

In study (I), it was demonstrated that for all three stimulation intensities the skin tissue was subjected to the greatest amount of stress compared with the other soft tissues. This confirms the protective role of skin layer for the deep structures [24]. It has been suggested that the sensitivity of nociceptors is more mechanically related to strain rather than stress [24] whereas it is still unknown which one of these mechanical factors contributes substantially to the pain sensitivity. From mechanical view point there is a direct relationship between the stress and strain in elastic materials [5]. However, this relationship in the soft tissues of human body (hyper-elastic materials with high non-linearity) is complicated [65]. Therefore, the elaboration of relationship among the pain response, stress, and strain needs additional and deep investigations.

The previous studies about the single-point algometry have shown that the probe design is an important factor in detection of painful threshold values [24,37,48]. The pressure pain thresholds were significantly lower using larger probes compared with the smaller probes [24]. Also, in single-point algometry the maximal stress generated in the muscle tissue had an increasing trend when using larger probes from 5 to 10, and 15 mm diameter rounded flat probe [24]. The findings of study (I) are in line with the results of single-point algometry and confirm that enlarging the area of stimulation increases the stress and strain values in deep tissue. The maximal stress and strain values in muscle tissue during the cuff algometry (study I) were 3.70 and 1.75 times greater than the highest value of stress and strain in the same tissue during the single-point algometry which was performed by the most efficient 15 mm diameter rounded flat probe [24]. These results prove the better capability of cuff algometry in terms of the magnitude of stress and strain values in deep tissue compared with single-point algometry.

The distribution of stress and strain is fundamentally different between the cuff algometry and single-point algometry. The maximum stress was always in correspondence with the probe perimeter in the flat and the center of the circle in the rounded probe stimulation [24]. Generally, in single-point algometry the stress is localized around the contact point of probe and tissue and consequently is not able to challenge the areas far from this site. However, the findings of study (I) show that the pattern of stress and strain distribution in cuff algometry is not restricted to the contact area. The simulations demonstrate that during the cuff compressions the stress and strain are originated from the regions around the bony structures and distributed toward the circumferential areas of muscle surface. This confirms that during the cuff algometry the areas with stress concentration are longitudinally found at the proximity of hard tissues and circumferentially in the cuff position area. Thus cuff algometry is a more efficient approach compared to the single-point algometry for challenging the deep tissues in terms of both the magnitude and distribution of stress and strain in deep tissue structures.

5.3. Mechanical effects of cuff stimulation on innervated layers (study II)

Periosteal tissues have the highest density of sensory innervation compared to marrow or mineralized bone [59]. It has been found that the mechanical [60] and chemical [36] stimulation of the periosteum are more painful and possess a significant lower threshold

compared to the adipose and muscle structures. The sensory innervating fibers of the periosteal layer are ideally located to participate in the development of bone-associated pain [22]. Also, human and animal investigations have shown that the external surface of the muscle tissue representing the fascial layer is densely innervated and highly sensitive [46,47,52]. The increased pain has also been demonstrated in response to hypertonic saline injection directed to fascial/epimysium tissue compared with muscle injection following eccentric exercise [30]. Furthermore, the pressure-evoked pain is highly dependent on mechanical excitation of nociceptors [34]. Thus the mechanical influences of cuff algometry on highly innervated layers e.g. periosteum and fascial tissue are of the most important factors involved in pressure-induced pain.

According to the findings of study (II) the muscle surface was subjected to the highest amount of strain and lowest amount of stress compared with the periosteal layers during the cuff compressions. The fascial layers are located between the soft tissues whereas the periosteum is in the vicinity of hard tissues and its displacement could be limited. This might explain the lower value of strain for periosteal layers. Also, higher amount of stress on the periosteal layers is supported by the theory of intensive mechanical stress which occurs at the proximity of geometric discontinuities [68].

The finite element modelling of single-point pressure algometry revealed that the smaller probe caused a larger area of the periosteum being strained compared with the larger probe [22]. In other words, larger probes mostly stimulate nociceptors of the muscle tissue while smaller diameter probes seem to be more effective to activate nociceptors in the periosteal layers [22]. In study (II), the lower strain values of the periosteal layers compared to the muscle surface tissue suggest that enlarging the area of external pressure stimulation from single-point stimulation to cuff stimulation cannot necessarily increase the ratio of periosteal strain to fascial strain ($\frac{\varepsilon_{\text{periost}}}{\varepsilon_{\text{fascia}}}$). On the other hand, assuming that strain is the ideal factor for mechanical stimulation of nociceptors [24], it could be hypothesized that cuff pressure stimulation may not be an appropriate approach for activation of nociceptors in the periosteal tissues whereas this kind of stimulation is more effective to challenge the nociceptors of fascial tissue.

5.4. Interface pressure behavior during cuff stimulation (study III)

The fundamental differences between the air-cuff and water-cuff systems are related to the magnitude and distribution of interface pressure around the limb. The results of study (III) showed a significant deviation between the amount of inflating pressure and interface pressure during the water-cuff algometry. However, this deviation is not observable while using air-cuff algometry. The pressure decline in water-cuff could be associated with different physical factors. The physical structure of the water-cuff prevents the mixture of water and air, causing a higher pressure to be needed to distribute the water inside the cuff to fill the uneven surfaces. Moreover, as the inflating pressure is increasing, an intimate contact is gradually established between the inner wall of the inflating water-cuff and the tissue [9] that may cause the water acts as a barrier such an incompressible ring between the compressed air and limb. Based on Young-Laplace equation the pressure difference between the two sides of a liquid interface is proportionally related to the surface tension of that liquid [8]. The high surface tension of water imposes a pressure loss between the inner and outer surfaces of water layer meaning that water layer resists pressure transfer to the limb surface. This could explain the dramatic decline of interface pressure value at high water-cuff compression intensities.

According to the results of study (III) the pattern of interface pressure distribution was generally heterogeneous. It has been proposed that the pressure gradient along the axial direction applied by cuff on the limb can generate shear effects inside the tissues [31]. The results of study (III) demonstrates a pressure gradient along the z-axis for both the air and water cuff which follows a bell-shaped profile peaking in the center of cuff and reaching minimum in the proximal and distal edges. Also, along the circumferential direction of the limb a two-dimensional finite element modeling of the transverse plane at the center of cuff has shown that a uniform pressure distribution is more effective than the non-uniform distribution in producing bulk deformations of the calf [64]. In study (III) a regular pattern was not observed for the location of the areas on the circumference of the limb which are subjected to the pressure concentration during air and water cuff algometry.

Nonetheless, the results of the analysis of standard deviation and entropy of interface pressure distribution generated by two types of cuff systems could be considered from several perspectives. The amount of standard deviation of interface pressure increased during both kinds of cuff algometry meaning that the variability of interface pressure distribution in air and water cuff algometry has an increasing trend over the cuff stimulation. This might be due

to the local increasing of pressure around the limb [50] leading into a more intermittent pattern of interface pressure at high cuff compression intensities. The increasing trend of entropy during both kinds of cuff algometry indicates that the homogeneity of interface pressure distribution decreases in air and water cuff systems during the inflating process. Two factors may be involved in this phenomenon. The limb is a biomechanically asymmetric system including different anatomical structures with different mechanical properties [38]. Therefore, the cuff does not necessarily deliver a uniform pressure to the limb [74] meaning that the mechanical interaction between the cuff and limb is not symmetric and becomes more irregular at high cuff compression intensities. Also, the restriction of cuff for expansion at higher pressure intensities could be another factor which gradually deteriorates the homogeneity of interface pressure distribution. It was also found that the variability and entropy of the pressure distribution of water-cuff is significantly less than air-cuff which should be taken into account as one of the fundamental differences between the two types of cuff systems. During the increasing trend of cuff compression, the water makes an interface layer between the compressed air and tissue. Since water is incompressible, this interface layer inhibits pressure transfer to the limb surface [8] and hence diminishes the mechanical interaction between the cuff and limb, causing a more homogeneous pressure distribution compared with the air-cuff system. The implications of this study suggest that using a liquid media in cuff systems improves the homogeneity of pressure distribution on the limb surface; however, the decline in the magnitude of interface pressure should be considered as one of the principal features of this methodology.

5.5. Modelling considerations

The mechanical properties of human soft tissues are subject-dependent and even change with respect to locations on a single subject [82]. The elastic properties of the soft tissues may vary with regard to age [14]. Thus, one of the limitations of this finite element simulation is related to the material parameters assigned to the tissues composing the model. More studies are needed to gather the experimental data and calibrate the bulk and shear modulus of Neo-Hookean or Mooney-Rivlin strain energy function for each subject independently. As the main focus of this study was to evaluate the general pattern of stress and strain distribution in deep-tissue, the high accuracy of the values of mechanical parameters of soft tissues was of limited interests. The sex differences are not simply associated with the mechanical properties

of soft tissue and their effects on activation of muscle nociceptors [21]. Therefore, the outcomes of present project were based on a single male subject and could be considered as a single case study providing fundamental information regarding the stress and strain analysis in different anatomical structures and clarifying methodological approach for FE simulation of the tissues during mechanically painful stimulations. Future studies should include several subjects to draw a general conclusion by comparing their data with outcomes of the present study.

In reality the living tissues are anisotropic and compressible [28] but their mechanical parameters are not available and in line with previous studies [19,21-25,83], these materials were assumed to be homogeneous and nearly incompressible. The compliance of various skeletal muscles is not equal among different muscle groups. For instance, the tibialis anterior muscle is hard and compact while the gastrocnemius muscle shows softer and bulkier properties [21]. The anatomical data shows that the lower limb contains connective tissues, e.g. fascia. The fascia may offer resistance against the energy of mechanical pressure propagation, causing more external load for adequate activation of peripheral nociceptors [66]. The different muscle groups, fascia, and nerves were modelled as one compartment in the simulation mainly due to unavailability of reliable mechanical parameters for the nerves, fascial tissue, and various muscle groups. Further studies considering all anatomical tissues based on reliable data of mechanical parameters are a potential to improve the current method.

The main reason for not expanding the current simulation study with more subjects was the extreme resource allocation which is required for three-dimensional finite element construction from magnetic resonance imaging. Three-dimensional segmentation of different anatomical structures and volumetric reconstruction of the limb are highly technical issues which should be performed by professional biomedical image processing software. One of the clear-cut distinctions between this study and previous studies [21-25,64] is the three-dimensional segmentation performed in this project for defining the geometry of each tissue in the space which is very complicated compared with two-dimensional segmentation. Moreover, from the view point of FE method, the number of dimensions of a model and also the number of non-linear materials included in the model are two significant factors determining complexity of the model, solution time, and convergence of the solution. To our knowledge, this is the first study that provides meaningful information about the stress and strain distribution extracted from the FE simulation of the real three-dimensional geometry of the lower leg based on three different kinds of non-linear tissues (skin, adipose and muscle)

composing the limb. Some of the previous FE modellings of the lower leg [64,83] were restricted to two-dimensional simulations due to the difficulties of three-dimensional segmentation and volumetric reconstructions. There are other studies [4,19] simulating three-dimensional FE model of the lower leg; however, their model include only two kinds of soft tissues (adipose and muscle). The three-dimensional modelling studies [21-25] which have considered the three kinds of soft tissues did not construct the real geometry of the limb and were based on extrusion of a single MRI slice along the longitudinal axis of the limb. In summary, this is the first inclusive study which has constructed the real three-dimensional geometry of the limb and also includes the most number of different kinds of soft tissues demonstrating the strengths of this study.

Chapter 6

Conclusions and implications

The proposed model in this project provided a new insight into the mechanical factors involved in painful cuff stimulations. Cuff algometry is more capable to mechanically stimulate muscle tissue in terms of the amount of stress and strain in contrast to the standard single-point pressure algometry. Also, the stress and strain are extensively distributed in muscle tissue compared to the localized distribution particularly occurring in the vicinity of probe contact area in single-point algometry. During cuff stimulations the periosteal layers in close proximity of the bony structures are mostly subjected to stress, whereas superficial muscle structures and fascial layers surrounding muscle tissue are mostly subjected to strain. Assuming strain as the ideal factor for stimulation of mechanonociceptors, it could be suggested that cuff pressure methodology is more appropriate for challenging the nociceptors of fascial tissue rather than periosteal layers. The characteristics of interface pressure on the limb surface are the key factors extrinsically involved in pain sensitivity assessment during cuff algometry. Cuff systems with liquid medium improve the distribution of interface pressure around the limb by decreasing the variability and increasing the homogeneity of this pressure whereas the deviation of the interface pressure value from cuff inflating pressure should be considered as one of the distinguishing features of this kind of cuff algometry.

These findings are highly relevant to clinical and biomechanical studies for defining a valid methodology to appropriately activate deep tissue nociceptors. This will lead to an improvement in the reliability of cuff algometry data obtained from pain sensitivity assessment in diagnostic procedure and pharmacological profiling studies. This project can separately be considered as a fundamental step in order to utilize the finite element method for investigation of the mechanical influences of pressure algometry on deep tissue structures during quantitative pain assessment.

6.1. Future perspectives

Future studies should be fundamentally oriented to ensure that which mechanical parameter i.e. stress or strain is significantly associated with pain response. More investigations should also be performed on different subjects based on their sex, age, and related parameters to

clarify the mechanical properties of tissues among different groups and consequently improving the modelling characteristics. Studies on the influences of repeated stimulations i.e. temporal summation on the deep-tissue stress and strain are of the considerable potentials which could complete the findings of this project. In addition, it should be investigated that which stimulation technique is efficiently able to elicit pain from the targeted anatomical structures e.g. muscle, periosteum, and fascia mainly contributing to pain generation. Based on this a specific protocol can be developed by involving both researchers and practitioners to provide strongly related clinical data for different groups of patients and situations.

References

1. Arendt-Nielsen L, Nie H, Laursen M B, Laursen B S, Madeleine P, Simonsen O H, Graven-Nielsen T (2010) Sensitization in patients with painful knee osteoarthritis. Pain 149:573-581

2. Arendt-Nielsen L. (1997) Induction and assessment of experimental pain from human skin, muscle, and viscera. :393-425

3. Auerbach S M. (1984) Axisymmetric finite element analysis of tourniquet application on limb. J Biomech 17:861-866

4. Avril S, Bouten L, Dubuis L, Drapier S, Pouget J (2010) Mixed experimental and numerical approach for characterizing the biomechanical response of the human leg under elastic compression. J Biomech Eng 132:031006

5. Beer F, Johnston E, DeWolf J (2002) Mechanics of Materials, 2002.

6. Borda, M. Fundamentals in information theory and coding. : Springer Science & Business Media, 2011

7. Breivik H, Collett B, Ventafridda V, Cohen R, Gallacher D (2006) Survey of chronic pain in Europe: prevalence, impact on daily life, and treatment. European journal of pain 10:287-287

8. Butt, H., K. Graf, and M. Kappl. Physics and chemistry of interfaces. : John Wiley & Sons, 2006

9. Casey V, O'sullivan S, McEwen J (2004) Interface pressure sensor for IVRA and other biomedical applications. Med Eng Phys 26:177-182

10. Ceelen K, Stekelenburg A, Mulders J, Strijkers G, Baaijens F, Nicolay K, Oomens C (2008) Validation of a numerical model of skeletal muscle compression with MR tagging: a contribution to pressure ulcer research. J Biomech Eng 130:061015

11. Chen, W. and D. Han. Plasticity for structural engineers. : J. Ross Publishing, 2007

12. Cherubini C, Filippi S, Nardinocchi P, Teresi L (2008) An electromechanical model of cardiac tissue: Constitutive issues and electrophysiological effects. Prog Biophys Mol Biol 97:562-573

13. Cheung J T, Zhang M, Leung A K, Fan Y (2005) Three-dimensional finite element analysis of the foot during standing—a material sensitivity study. J Biomech 38:1045-1054

14. Cua A, Wilhelm K, Maibach H (1990) Elastic properties of human skin: relation to age, sex, and anatomical region. Arch Dermatol Res 282:283-288

15. Dai G, Gertler J, Kamm R (1999) The effects of external compression on venous blood flow and tissue deformation in the lower leg. J Biomech Eng 121:557-564

16. Daly C H and Odland G F (1979) Age-related changes in the mechanical properties of human skin. J Invest Dermatol 73:84-87

17. Delaney A, Fleetwood-Walker S M, Colvin L A, Fallon M (2008) Translational medicine: cancer pain mechanisms and management. Br J Anaesth 101:87-94

18. Dorner T E, Muckenhuber J, Stronegger W J, Ràsky É, Gustorff B, Freidl W (2011) The impact of socio-economic status on pain and the perception of disability due to pain. European Journal of Pain 15:103-109

19. Dubuis L, Avril S, Debayle J, Badel P (2012) Identification of the material parameters of soft tissues in the compressed leg. Comput Methods Biomech Biomed Engin 15:3-11

20. Fabio Antonaci M. (1998) Pressure algometry in healthy subjects: inter-examiner variability. Scand J Rehab Med 30:3-8

21. Finocchietti S, Takahashi K, Okada K, Watanabe Y, Graven-Nielsen T, Mizumura K (2013) Deformation and pressure propagation in deep tissue during mechanical painful pressure stimulation. Med Biol Eng Comput 51:113-122

22. Finocchietti S, Andresen T, Arendt-Nielsen L, Graven-Nielsen T (2012) Pain evoked by pressure stimulation on the tibia bone–influence of probe diameter on tissue stress and strain. European Journal of Pain 16:534-542

23. Finocchietti S, Arendt-Nielsen L, Graven-Nielsen T (2012) Tissue characteristics during temporal summation of pressure-evoked pain. Experimental brain research 219:255-265

24. Finocchietti S, Nielsen M, Mørch C D, Arendt-Nielsen L, Graven-Nielsen T (2011) Pressure-induced muscle pain and tissue biomechanics: A computational and experimental study. European Journal of Pain 15:36-44

25. Finocchietti S, Morch C D, Arendt-Nielsen L, Graven-Nielsen T (2011) Effects of adipose thickness and muscle hardness on pressure pain sensitivity. Clin J Pain 27:414-424

26. Fischer A A. (1987) Pressure algometry over normal muscles. Standard values, validity and reproducibility of pressure threshold. Pain 30:115-126

27. Friessem C H, Willweber-Strumpf A, Zenz M W (2009) Chronic pain in primary care. German figures from 1991 and 2006. BMC Public Health 9:299-2458-9-299

28. Fung Y. Biomechanics: mechanical properties of living tissues. 1993. New York, NY

29. Gerdle B, Bjork J, Henriksson C, Bengtsson A (2004) Prevalence of current and chronic pain and their influences upon work and healthcare-seeking: a population study. J Rheumatol 31:1399-1406

30. Gibson W, Arendt-Nielsen L, Taguchi T, Mizumura K, Graven-Nielsen T (2009) Increased pain from muscle fascia following eccentric exercise: animal and human findings. Experimental brain research 194:299-308

31. Graham B, Breault M J, McEwen J A, McGraw R W (1992) Perineural pressures under the pneumatic tourniquet in the upper extremity. J Hand Surg Br 17:262-266

32. Graven-Nielsen T and Arendt-Nielsen L (2010) Assessment of mechanisms in localized and widespread musculoskeletal pain. Nature Reviews Rheumatology 6:599-606

33. Graven-Nielsen T. (2006) Fundamentals of muscle pain, referred pain, and deep tissue hyperalgesia. Scand J Rheumatol 35:1-43

34. Graven-Nielsen T, Mense S, Arendt-Nielsen L (2004) Painful and non-painful pressure sensations from human skeletal muscle. Experimental brain research 159:273-283

35. Graven-Nielsen T and Mense S (2001) The peripheral apparatus of muscle pain: evidence from animal and human studies. Clin J Pain 17:2-10

36. Graven-Nielsen T, Arendt-Nielsen L, Svensson P, Jensen T S (1997) Experimental muscle pain: a quantitative study of local and referred pain in humans following injection of hypertonic saline. Journal of Musculoskelatal Pain 5:49-69

37. Greenspan J D and McGillis S L (1991) Stimulus features relevant to the perception of sharpness and mechanically evoked cutaneous pain. Somatosens Mot Res 8:137-147

38. Griffiths J and Heywood O (1973) Bio-mechanical aspects of the tourniquet. Hand 5:113-118

39. Grönblad M, Liesi P, Korkala O, Karaharju E, Polak J (1984) Innervation of human bone periosteum by peptidergic nerves. Anat Rec 209:297-299

40. Hasselström J, Liu-Palmgren J, Rasjö-Wrååk G (2002) Prevalence of pain in general practice. European journal of pain 6:375-385

41. Henry J L. (2008) The need for knowledge translation in chronic pain. Pain Res Manag 13:465-476

42. Hockaday J M and Whitty C W (1967) Patterns of referred pain in the normal subject. Brain 90:481-496

43. Honore P and Mantyh P W (2000) Bone cancer pain: from mechanism to model to therapy. Pain Medicine 1:303-309

44. Humphrey J. (2003) Review Paper: Continuum biomechanics of soft biological tissues. 459:3-46

45. Irgens, F. Continuum mechanics. : Springer Science & Business Media, 2008

46. Itoh K and Kawakita K (2002) Effect of indomethacin on the development of eccentric exercise-induced localized sensitive region in the fascia of the rabbit. The Japanese journal of physiology 52:173-180

47. Itoh K, Okada K, Kawakita K (2004) A proposed experimental model of myofascial trigger points in human muscle after slow eccentric exercise. Acupunct Med 22:2-12; discussion 12-3

48. Jensen K, Andersen H Ø, Olesen J, Lindblom U (1986) Pressure-pain threshold in human temporal region. Evaluation of a new pressure algometer. Pain 25:313-323

49. Jespersen A, Dreyer L, Kendall S, Graven-Nielsen T, Arendt-Nielsen L, Bliddal H, Danneskiold-Samsoe B (2007) Computerized cuff pressure algometry: a new method to assess deep-tissue hypersensitivity in fibromyalgia. Pain 131:57-62

50. John G W, Morris R, Woodcock J, Narracott A, Lawford P V, Hose D R (2007) Influence of intermittent compression cuff design on interface pressure and calf deformation: experimental results. :2122-2125

51. Kasch H, Qerama E, Bach F W, Jensen T S (2005) Reduced cold pressor pain tolerance in non-recovered whiplash patients: a 1-year prospective study. European Journal of Pain 9:561-561

52. Kawakita K, Miura T, Iwase Y (1991) Deep pain measurement at tender points by pulse algometry with insulated needle electrodes. Pain 44:235-239

53. Kellgren J. (1938) Observations on referred pain arising from muscle. Clin Sci 3:1937-1938

54. Kumazawa T and Mizumura K (1977) Thin-fibre receptors responding to mechanical, chemical, and thermal stimulation in the skeletal muscle of the dog. J Physiol (Lond) 273:179-194

55. Kurihashi A, Tamai K, Saotome K, Takemura M, Fujiwara A, Fujita S (2006) Difference in stretching of sarcomeres between medial gastrocnemius and tibialis anterior by tibial lengthening: an experiment in rabbits. Journal of Orthopaedic Surgery 14

56. Latham J and Davis B (1994) The socioeconomic impact of chronic pain. Disability & Rehabilitation 16:39-44

57. Lewis T. (1938) Study of Somatic Pain. Br Med J 1:321-325

58. Lubliner, J. Plasticity theory. : Courier Corporation, 2008

59. Mach D, Rogers S, Sabino M, Luger N, Schwei M, Pomonis J, Keyser C, Clohisy D, Adams D, O'leary P (2002) Origins of skeletal pain: sensory and sympathetic innervation of the mouse femur. Neuroscience 113:155-166

60. Martin C D, Jimenez-Andrade J M, Ghilardi J R, Mantyh P W (2007) Organization of a unique net-like meshwork of CGRP sensory fibers in the mouse periosteum: implications for the generation and maintenance of bone fracture pain. Neurosci Lett 427:148-152

61. Mense S. (1993) Nociception from skeletal muscle in relation to clinical muscle pain. Pain 54:241-289

62. Milne R, Aniss A, Kay N, Gandevia S (1988) Reduction in perceived intensity of cutaneous stimuli during movement: a quantitative study. Experimental Brain Research 70:569-576

63. Mooney M. (1940) A theory of large elastic deformation. J Appl Phys 11:582-592

64. Narracott A J, John G W, Morris R J, Woodcock J P, Hose D R, Lawford P V (2009) A validated model of calf compression and deep vessel collapse during external cuff inflation. Biomedical Engineering, IEEE Transactions on 56:273-280

65. Ogden, R. W. Non-linear elastic deformations. : Courier Corporation, 1997

66. Ohrbach R and Gale E N (1989) Pressure pain thresholds in normal muscles: reliability, measurement effects, and topographic differences. Pain 37:257-263

67. Parry D A, Barnes G R, Craig A S (1978) A comparison of the size distribution of collagen fibrils in connective tissues as a function of age and a possible relation between fibril size distribution and mechanical properties. Proc R Soc Lond B Biol Sci 203:305-321

68. Peterson R E. (1953) Stress concentration design factors.

69. Polianskis R, Graven-Nielsen T, Arendt-Nielsen L (2002) Spatial and temporal aspects of deep tissue pain assessed by cuff algometry. Pain 100:19-26

70. Polianskis R, Graven-Nielsen T, Arendt-Nielsen L (2001) Computer-controlled pneumatic pressure algometry—a new technique for quantitative sensory testing. European Journal of Pain 5:267-277

71. Rolke R, Campbell K A, Magerl W, Treede R (2005) Deep pain thresholds in the distal limbs of healthy human subjects. European Journal of Pain 9:39-48

72. Sandrini G, Antonaci F, Pucci E, Bono G, Nappi G (1994) Comparative study with EMG, pressure algometry and manual palpation in tension-type headache and migraine. Cephalalgia 14:451-7; discussion 394-5

73. Silber, G. and C. Then. Preventive Biomechanics: Optimizing Support Systems for the Human Body in the Lying and Sitting Position. : Springer Science & Business Media, 2012

74. SINCLAIR D C. (1948) Observations on sensory paralysis produced by compression of a human limb. J Neurophysiol 11:75-92

75. Skou S T, Graven-Nielsen T, Rasmussen S, Simonsen O H, Laursen M B, Arendt-Nielsen L (2013) Widespread sensitization in patients with chronic pain after revision total knee arthroplasty. Pain 154:1588-1594

76. Sleed M, Eccleston C, Beecham J, Knapp M, Jordan A (2005) The economic impact of chronic pain in adolescence: methodological considerations and a preliminary costs-of-illness study. Pain 119:183-190

77. Spencer, A. J. M. Continuum mechanics. : Courier Corporation, 2004

78. Sterling M, Treleaven J, Edwards S, Jull G (2002) Pressure pain thresholds in chronic whiplash associated disorder: further evidence of altered central pain processing. Journal of Musculoskelatal Pain 10:69-81

79. Svensson P and Arendt-Nielsen L (1995) Induction and assessment of experimental muscle pain. Journal of Electromyography and Kinesiology 5:131-140

80. Timoshenko, S. Strength of materials. : New York, 1930

81. Tran H, Charleux F, Rachik M, Ehrlacher A, Ho Ba Tho M (2007) In vivo characterization of the mechanical properties of human skin derived from MRI and indentation techniques. Comput Methods Biomech Biomed Engin 10:401-407

82. Vannah W M and Childress D S (1996) Indentor tests and finite element modeling of bulk muscular tissue in vivo. Journal of rehabilitation research and development 33:239-252

83. Wang Y, Downie S, Wood N, Firmin D, Xu X Y (2013) Finite element analysis of the deformation of deep veins in the lower limb under external compression. Med Eng Phys 35:515-523

84. Weddell G and Harpman J A (1940) The Neurohistological Basis for the Sensation of Pain Provoked from Deep Fascia, Tendon, and Periosteum. J Neurol Psychiatry 3:319-328

85. Willweber-Strumpf A, Zenz M, Bartz D (2000) Epidemiologie chronischer Schmerzen. Der Schmerz 14:84-91

86. Woolf A D, Erwin J, March L (2012) The need to address the burden of musculoskeletal conditions. Best practice & research Clinical rheumatology 26:183-224

Author CV

Bahram Manafi Khanian received the bachelor degree in Mechanical Engineering (Solid Mechanics) from K.N.Toosi University of Technology, Tehran, Iran and the master degree in Biomedical Engineering (Biomechanics) from Iran University of Science and Technology (IUST), Tehran, Iran where he performed pioneering researches on mechanics of brain injury during head impact via finite element method.

His research interests include Computational Biomechanics, Finite Element simulation, Tissue mechanics, Brain Biomechanics, Mathematical Modeling, and Functionality of biomedical devices.

SUMMARY

Cuff algometry is used for quantitative assessment of deep-tissue sensitivity. The main purpose of this PhD dissertation is to provide a novel insight into the intrinsic and extrinsic factors which are involved in mechanically induced pain during cuff pressure algometry. A computational 3D finite element of the lower leg representing the real geometry of the limb and including various soft tissues was developed based on magnetic resonance image data. Due to the technical difficulties of such a simulation and the beneficial aspects of the results, the contribution of this project is substantial to expand the current knowledge on the mechanical influences of cuff algometry on deep-tissue nociceptors. Additionally, this is one of the pioneering projects utilizing the finite element simulation as a computationally reliable method of modelling in pain research field. The present findings are highly relevant to biomechanical studies for defining a valid methodology to appropriately activate deep-tissue nociceptors and hence to develop biomedical devices used for pain sensitivity assessment.

ISSN (online): 2246-1302
ISBN (online): 978-87-7112-343-2

AALBORG UNIVERSITY PRESS